SIAM J. SCI. COMPUT.
Vol. 41, No. 5, pp. B929–B952

ON AN INVERSE SOURCE PROBLEM FOR THE FULL RADIATIVE TRANSFER EQUATION WITH INCOMPLETE DATA*

ALEXEY V. SMIRNOV†, MICHAEL V. KLIBANOV†, AND LOC H. NGUYEN†

Abstract. A new numerical method to solve an inverse source problem for the radiative transfer equation involving the absorption and scattering terms, with incomplete data, is proposed. No restrictive assumption on those absorption and scattering coefficients is imposed. The original inverse source problem is reduced to boundary value problem for a system of coupled partial differential equations of the first order. The unknown source function is not a part of this system. Next, we write this system in the fully discrete form of finite differences. That discrete problem is solved via the quasi-reversibility method. We prove the existence and uniqueness of the regularized solution. Especially, we prove the convergence of regularized solutions to the exact one as the noise level in the data tends to zero via a new discrete Carleman estimate. Numerical simulations demonstrate good performance of this method even when the data are highly noisy.

Key words. radiative transfer equation, absorption term, scattering term, inverse source problem, discrete Carleman estimate, quasi-reversibility method

AMS subject classification. 35R30

DOI. 10.1137/19M1253605

1. Introduction.

The stationary radiative transfer equation (RTE) is commonly used in optics, tomography, astrophysics, atmospheric science, and remote sensing to describe the propagation of the radiation field in media with absorbing, emitting, and scattering radiation. A significant number of studies is dedicated to the recovery of the parameters of the observed objects from the measured data, i.e., to the solutions of the inverse source problems (ISOPs) [1, 24] and coefficient inverse problems (CIPs) [2, 33]. A number of inverse problems may be formulated, depending on the object's parameters of interest.

The first reconstruction formula for the problem of the attenuated tomography was obtained by Novikov [31]. We also refer to [3, 12, 29] for reconstruction formulas as well as to [10, 29] for numerical results for the attenuated tomography with complete data and with the scattering phase function $K \equiv 0$. Uniqueness and stability results for similar ISOPs with complete data were obtained in [3, 34]. It was assumed in [3] that $|K|$ is sufficiently small. The assumption of [34] is that functions σ and K belong to certain dense sets of some function spaces. The scattering phase function K is involved in RTEs as the kernel of a certain integral operator, the attenuation coefficient is $\sigma = \mu_a + \mu_s$, where μ_a and μ_s are the absorption and scattering coefficients, respectively; see section 2.

In this paper, we propose a new numerical approach for the ISOP with limited angle data for the stationary RTE and prove its convergence. This is *the first publication,* in which a rigorously derived numerical method for the ISOP for the RTE does not use any restrictive assumptions neither on μ_a, nor on μ_s, nor on K, except the

*Submitted to the journal's Computational Methods in Science and Engineering section April 2, 2019; accepted for publication (in revised form) June 25, 2019; published electronically September 12, 2019.

https://doi.org/10.1137/19M1253605

Funding: This work was supported by U.S. Army Research Laboratory and U.S. Army Research Office grant W911NF-19-1-0044. The work of the third author was supported by The University of North Carolina at Charlotte through grant FRG 111172.

†Department of Mathematics and Statistics, University of North Carolina Charlotte, Charlotte, NC 28223 (asmirno2@uncc.edu, mklibanv@uncc.edu, loc.nguyen@uncc.edu).

smoothness and the requirement that functions μ_a and μ_s are compactly supported. Also, for the first time, a *discrete* Carleman estimate is applied here for the convergence analysis of an inverse problem. We note that discrete Carleman estimates are very rare, unlike the continuous ones. In addition, we prove the Lipschitz stability and uniqueness for our statement of the ISOP.

Our method is based on the solution of an overdetermined boundary value problem for a linear system of coupled integro-differential equations, in which the unknown source function is not present. The solution of this problem directly yields the solution of the desired ISOP. A similar idea was recently used in [23]. However, unlike the current paper, a quite restrictive condition $\sigma \equiv K \equiv 0$ is imposed in [23]. The ISOP for the RTE with limited angle data has many applications in optical imaging and tomography, such as bioluminescence tomography [13] and X-ray computerized tomography [27, 28].

The idea of our numerical method has roots in the Bukhgeim-Klibanov method (BK) [9]. BK was originally proposed in 1981 only for proofs of global uniqueness and stability results for CIPs for PDEs, rather than for numerical methods. BK is based on Carleman estimates. Since the current paper is not a survey of BK, we refer here only to a few publications about BK [5, 6, 15, 16, 17] and references cited therein. Currently, the idea of BK is extensively used for constructions of globally convergent numerical methods for CIPs for PDEs; see, e.g., [4, 18, 21, 22].

The second important element of our numerical method is the new orthonormal basis in the space $L^2(a,b), (a,b) \subset \mathbb{R}$, which was recently introduced in [20]. This basis has proven to be effective for numerical studies [21, 22, 23]. We use a truncated Fourier series with respect to this basis. We estimate an optimal number of terms of this series numerically and assume that this approximation still satisfies the RTE, i.e., we work with an *approximate mathematical model*; also, see Remarks 4.3 (section 4) and 5.7 (section 5).

We solve the above-mentioned overdetermined boundary value problem by the quasi-reversibility method (QRM), which is known to be effective to solve overdetermined boundary value problems. We consider a fully discrete form of our system, which is similar to what we use in the numerical tests. Next, we establish a new discrete Carleman estimate and use it to prove uniqueness and existence of the regularized solution for the QRM in the fully discrete form, in which partial derivatives with respect to spatial variables are written via finite differences. This Carleman estimate is also used to establish the convergence rate of regularized solutions. Finally, we conduct numerical testing for several different regimes of absorption and scattering to show the method's potential for solving problems in real-world tomography.

The QRM was originally introduced by Lattes and Lions in 1969 [25]. We also refer to, e.g., [7, 8, 12, 23] for this method. The second author has shown in the survey paper [19] that as long as a proper Carleman estimate for an ill-posed problem for a linear PDE is available, the convergent QRM can be constructed for this problem.

For brevity, we consider in this paper only the two-dimensional (2D) case. The considerations in the three-dimensional (3D) case are similar. We state both forward and inverse problems in section 2. In section 3 we derive the above-mentioned overdetermined boundary value problem for a system of coupled PDEs of the first order. To solve this problem, we apply the QRM by stating a minimization problem. In section 4 we introduce the fully discrete version of the QRM to solve that problem. Next, we derive a new discrete Carleman estimate. This estimate is used in section 5 to prove the existence and uniqueness of the minimizer of the QRM and also to establish the convergence rate of the minimizers to the exact solution as the level of noise in the

measured data tends to zero. Section 6 is devoted to numerical studies. Everywhere below we work only with real-valued functions.

2. Statements of forward and inverse problems. Let $\mathbf{x} = (x, y)$ denote an arbitrary point in $\mathbb{R}^2$. Let a, b, d, and R be the positive numbers, where $1 < a < b$ and $d \geq R$. Define the rectangular domain $\Omega \subset \mathbb{R}^2$ (Figure 2.1) as

$$\Omega = \{(x, y) : -R < x < R, a < y < b\}. \tag{2.1}$$

Let Γ_d be the line with external "sources"

$$\Gamma_d = \{\mathbf{x}_\alpha = (\alpha, 0) : \alpha \in [-d, d]\}. \tag{2.2}$$

Let $u(\mathbf{x}, \alpha)$ denote the steady-state radiance at the point $\mathbf{x}$ generated by the external source located at $\mathbf{x}_\alpha = (\alpha, 0) \in \Gamma_d$. Then, the function $u(\mathbf{x}, \alpha)$ satisfies the following RTE (see, e.g., [11]):

$$\nu(\mathbf{x}, \alpha) \cdot \nabla_{\mathbf{x}} u(\mathbf{x}, \alpha) + (\mu_a(\mathbf{x}) + \mu_s(\mathbf{x}))u(\mathbf{x}, \alpha) = \mu_s(\mathbf{x}) \int_{\Gamma_d} K(\mathbf{x}, \alpha, \beta)u(\mathbf{x}, \beta)d\beta + f(\mathbf{x}) \quad \text{for all } \mathbf{x} \in \Omega. \tag{2.3}$$

In the equation above, the function $f(\mathbf{x}) \in L^2(\mathbb{R}^2)$ is called the source function while the functions $\mu_a(\mathbf{x})$, $\mu_s(\mathbf{x}) \in C^1(\mathbb{R}^2)$ denote the absorption and scattering coefficients, respectively. We assume that

$$\mu_a(\mathbf{x}) = \mu_s(\mathbf{x}) = f(\mathbf{x}) = 0 \quad \text{for all } \mathbf{x} \in \mathbb{R}^2 \setminus \Omega. \tag{2.4}$$

The function $K(\mathbf{x}, \alpha, \beta) \in C^1(\mathbb{R}^2 \times [-d, d]^2)$ represents the so-called scattering phase function. The scattering phase function is the probability density of a particle scattering from the $\nu(\mathbf{x}, \beta)$-direction into the $\nu(\mathbf{x}, \alpha)$-direction. As the probability density,

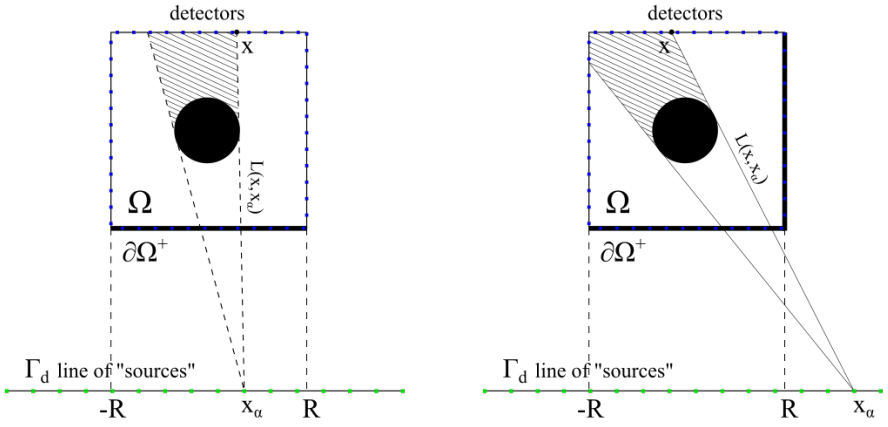

(a) The source/detector configuration of the problem in the case when the source is located at $\mathbf{x}_\alpha$ with $|\mathbf{x}_\alpha| < R$.

(b) The source/detector configuration of the problem in the case when the source is located at $\mathbf{x}_\alpha$ with $|\mathbf{x}_\alpha| > R$.

FIG. 2.1. *A schematic diagram of measurements for the 2D case. $L(\mathbf{x}, \mathbf{x}_\alpha)$ is a straight line, connecting the detector $\mathbf{x}$ with the source $\mathbf{x}_\alpha$.*

$K(\mathbf{x}, \alpha, \beta)$ possesses the following properties, discussed in detail in [11],

$$K(\mathbf{x}, \alpha, \beta) \geq 0, \quad \int_{\Gamma_d} \int_{\Gamma_d} K(\mathbf{x}, \alpha, \beta) d\alpha d\beta = 1. \tag{2.5}$$

Finally, $\nu(\mathbf{x}, \alpha)$ is the $\mathbb{R}^2$-vector, showing the direction of particles propagating from the external source located at $\mathbf{x}_\alpha = (\alpha, 0)$ to $\mathbf{x}$,

$$\nu(\mathbf{x}, \alpha) = \left(\frac{x - \alpha}{|\mathbf{x} - \mathbf{x}_\alpha|}, \frac{y}{|\mathbf{x} - \mathbf{x}_\alpha|} \right) = (\nu_1(\mathbf{x}, \alpha), \nu_2(\mathbf{x}, \alpha)) \tag{2.6}$$

for all $x \in [-R, R], y \in [a, b], \alpha \in [-d, d]$.

For a fixed α, let

$$\partial\Omega^+ = \{\mathbf{x} \in \partial\Omega : \nu(\mathbf{x}, \alpha) \cdot \mathbf{n}(\mathbf{x}) \leq 0\},$$

where $\mathbf{n}(\mathbf{x})$ is the unit outward normal vector at $\partial\Omega$ at point $\mathbf{x}$. Assuming that all functions in (2.3), except $u(\mathbf{x}, \alpha)$, are known in Ω, we formulate the following forward problem.

PROBLEM 2.1 (forward problem). *For each $\alpha \in [-d, d]$, find the function $u(\mathbf{x}, \alpha)$ satisfying* (2.3) *in the domain Ω as well as the following boundary condition:*

$$u(\mathbf{x}, \alpha) = 0 \quad \textit{for all } \mathbf{x} \in \partial\Omega^+. \tag{2.7}$$

In the appendix we prove existence and uniqueness of the solution of the boundary value problem (2.3), (2.7) and, moreover, discuss a numerical method to solve it. Conversely, assume now that the function $f(\mathbf{x})$ is unknown and the information of $u(\mathbf{x}, \alpha)$ on $\partial\Omega$ is known. The main goal of this paper is to numerically solve the following ISOP.

PROBLEM 2.2 (ISOP). *Assume that* (2.3) *and conditions* (2.4), (2.5) *hold. Also, let the vector $\nu(\mathbf{x}, \alpha)$ in* (2.3) *have the form* (2.6). *Reconstruct the function $f(\mathbf{x})$, $\mathbf{x} \in \Omega$, given the following boundary data $Z(\mathbf{x}, \alpha)$:*

$$Z(\mathbf{x}, \alpha) = u(\mathbf{x}, \alpha) \quad \textit{for all } \mathbf{x} \in \partial\Omega, \alpha \in [-d, d], \tag{2.8}$$

where $u(\mathbf{x}, \alpha)$ is the solution of Problem 2.1 *and*

$$Z(\mathbf{x}, \alpha) = 0 \textit{ for } \mathbf{x} \in \partial\Omega^+. \tag{2.9}$$

Remark 2.3. In the particular case when $\mu_a(\mathbf{x}) \equiv \mu_s(\mathbf{x}, \alpha) \equiv 0$, this ISOP is exactly the problem of x-ray tomography with incomplete data, which was considered in [23]. However, the main focus of the current paper is to develop a numerical method for this problem allowing the presence of μ_a, μ_s, K in the case when restrictive technical conditions are not imposed on these terms.

3. Numerical method for the ISOP.

3.1. An orthonormal basis in $L^2(-d, d)$. First, we recall a special orthonormal basis in the space $L^2(-d, d)$, which was introduced in [20]. For $\alpha \in [-d, d]$ consider the set of linearly independent functions $\{\alpha^{n-1} e^\alpha\}_{n=1}^\infty$. These functions form a complete set in $L^2(-d, d)$. Applying the classical Gram–Schmidt orthonormalization procedure to this set, we obtain the orthonormal basis $\{\Psi_n(\alpha)\}_{n=1}^\infty$ in $L^2(-d, d)$. This basis has the following properties [20]:

1. The functions $\Psi_n \in C^1[-d,d]$ and $\Psi_n'(\alpha)$ are not identically 0 for all $n = 1,2,\dots$.
2. $a_{nn} = 1$ and $a_{mn} = 0$ for all $m,n = 1,2,\dots$ such that $n < m$, where

$$a_{mn} = \int_{-d}^{d} \Psi_n'(\alpha)\Psi_m(\alpha)d\alpha = \begin{cases} 1 & \text{if } m = n, \\ 0 & \text{if } m > n. \end{cases}$$

Item 2 implies that the matrix

$$M_N = (a_{mn})_{m,n=1}^{N} \tag{3.1}$$

is invertible for all $N = 1,2,\dots$.

Hence, the function $u(\mathbf{x},\alpha)$ can be written as the following Fourier series converging in $L^2(-d,d)$ for every point $\mathbf{x} \in \overline{\Omega}$:

$$u(\mathbf{x},\alpha) = \sum_{n=1}^{\infty} u_n(\mathbf{x})\Psi_n(\alpha) \quad \text{for all } \alpha \in [-d,d],$$

where

$$u_n(\mathbf{x}) = \int_{-d}^{d} u(\mathbf{x},\alpha)\Psi_n(\alpha)d\alpha.$$

We approximate the function $u(\mathbf{x},\alpha)$ via the following truncated Fourier series:

$$u(\mathbf{x},\alpha) \approx \sum_{n=1}^{N} u_n(\mathbf{x})\Psi_n(\alpha), \quad \mathbf{x} \in \overline{\Omega}, \quad \alpha \in [-d,d], \tag{3.2}$$

where $N \geq 1$ is a certain integer, which is chosen numerically. Furthermore, we assume that differentiating the right-hand side of (3.2) with respect to the parameter α, we obtain a good approximation for the α-derivative $\partial_\alpha u(\mathbf{x},\alpha)$ of the true function $u(\mathbf{x},\alpha)$. It is convenient to denote this derivative as $\partial_\alpha u(\mathbf{x},\alpha) := u_\alpha(\mathbf{x},\alpha)$. Thus, we assume that, in addition to (3.2),

$$u_\alpha(\mathbf{x},\alpha) \approx \sum_{n=1}^{N} u_n(\mathbf{x})\Psi_n'(\alpha), \quad \mathbf{x} \in \overline{\Omega}, \quad \alpha \in [-d,d]. \tag{3.3}$$

We assume that the truncated series (3.2) satisfies (2.3). In addition, we assume that both sides of the equation resulting after the substitution of (3.2) in (2.3) can be differentiated with respect to the parameter α as in (3.3); see Remark 4.3.

3.2. A coupled system of first-order differential equations. Just as in the first step of the above mentioned BK method [9], we eliminate the unknown source function $f(\mathbf{x})$ from (2.3) via the differentiation of that equation with respect to the parameter α from which $f(\mathbf{x})$ does not depend. We obtain

$$\nu(x,y,\alpha)\cdot\nabla u_\alpha - \frac{y^2}{|\mathbf{x}-\mathbf{x}_\alpha|^3}u_x + \frac{(x-\alpha)y}{|\mathbf{x}-\mathbf{x}_\alpha|^3}u_y + (\mu_a+\mu_s)(\mathbf{x})\,u_\alpha - \mu_s(\mathbf{x})\int_{\Gamma_d} K_\alpha(\mathbf{x},\alpha,\beta)u(\mathbf{x},\beta)d\beta = 0 \tag{3.4}$$

for all $\mathbf{x} = (x, y) \in \Omega$. Multiplying (3.4) by $|\mathbf{x} - \mathbf{x}_\alpha|/y$, we obtain

$$
\begin{aligned}
(3.5)\qquad & u_{y,\alpha} + \frac{x-\alpha}{y} u_{x,\alpha} + \frac{y}{|\mathbf{x}-\mathbf{x}_\alpha|^2} u_x + \frac{(x-\alpha)}{|\mathbf{x}-\mathbf{x}_\alpha|^2} u_y \\
& + \frac{|\mathbf{x}-\mathbf{x}_\alpha|}{y} \left[(\mu_a + \mu_s)(\mathbf{x})\, u_\alpha - \mu_s(\mathbf{x}) \int_{\Gamma_d} K_\alpha(\mathbf{x}, \alpha, \beta) u(\mathbf{x}, \beta) d\beta \right] = 0.
\end{aligned}
$$

Substituting representations (3.2) and (3.3) into (3.5), multiplying the resulting equation by functions $\Psi_m(\alpha)$ for each $m \in \{1, 2, \ldots, N\}$, we obtain

$$
\begin{aligned}
(3.6)\qquad & \sum_{n=1}^{N} \frac{\partial u_n}{\partial y} \Psi_n'(\alpha) \Psi_m(\alpha) + \frac{x-\alpha}{y} \sum_{n=1}^{N} \frac{\partial u_n}{\partial x} \Psi_n'(\alpha) \Psi_m(\alpha) \\
& + \frac{y}{|\mathbf{x}-\mathbf{x}_\alpha|^2} \sum_{n=1}^{N} \frac{\partial u_n}{\partial x} \Psi_n(\alpha) \Psi_m(\alpha) + \frac{(x-\alpha)}{|\mathbf{x}-\mathbf{x}_\alpha|^2} \sum_{n=1}^{N} \frac{\partial u_n}{\partial y} \Psi_n(\alpha) \Psi_m(\alpha) \\
& + \frac{|\mathbf{x}-\mathbf{x}_\alpha|}{y} \Psi_m(\alpha) \sum_{n=1}^{N} \left[(\mu_a + \mu_s)(\mathbf{x})\, u_n \Psi_n'(\alpha) \right] \\
& - \frac{|\mathbf{x}-\mathbf{x}_\alpha|}{y} \Psi_m(\alpha) \sum_{n=1}^{N} \left[\mu_s(\mathbf{x}) \int_{\Gamma_d} K_\alpha(\mathbf{x}, \alpha, \beta) u_n(\mathbf{x}) \Psi_n(\beta)\, d\beta \right] = 0.
\end{aligned}
$$

Integrate (3.6) with respect to $\alpha \in (-d, d)$. Recalling the definition of the matrix M_N in (3.1), we obtain

$$
(3.7)\qquad M_N U_y = \mathbf{A} U_y + \mathbf{B} U_x + \mathbf{C} U, \quad U(\mathbf{x}) = (u_1(\mathbf{x}), \ldots, u_N(\mathbf{x}))^T.
$$

Here $\mathbf{A}$, $\mathbf{B}$, and $\mathbf{C}$ are $N \times N$ matrices with the following entries:

$$
(3.8)\qquad (\mathbf{A})_{mn} = \int_{\Gamma_d} \frac{(x-\alpha)}{|\mathbf{x}-\mathbf{x}_\alpha|^2} \Psi_n(\alpha) \Psi_m(\alpha) d\alpha,
$$

$$
(3.9)\qquad (\mathbf{B})_{mn} = \int_{\Gamma_d} \left[\frac{x-\alpha}{y} \Psi_n'(\alpha) \Psi_m(\alpha) + \frac{y}{|\mathbf{x}-\mathbf{x}_\alpha|^2} \Psi_n(\alpha) \Psi_m(\alpha) \right] d\alpha,
$$

$$
\begin{aligned}
(3.10)\qquad (\mathbf{C})_{mn} = & \int_{\Gamma_d} \frac{|\mathbf{x}-\mathbf{x}_\alpha|}{y} (\mu_a + \mu_s)(\mathbf{x})\, \Psi_n'(\alpha) \Psi_m(\alpha) d\alpha \\
& - \int_{\Gamma_d} \frac{|\mathbf{x}-\mathbf{x}_\alpha|}{y} \mu_s(\mathbf{x}) \left(\int_{\Gamma_d} K_\alpha(\mathbf{x}, \alpha, \beta) \Psi_n(\beta)\, d\beta \right) \Psi_m(\alpha) d\alpha.
\end{aligned}
$$

Everywhere below the norm of a matrix is the square root of the sum of square norms of its entries. Since in the definition of the domain Ω the number $a > 1$, the following estimates follow from (3.8)–(3.10):

$$
\max_{\mathbf{x} \in \overline{\Omega}} \|\mathbf{A}(\mathbf{x})\| \le \frac{C_0}{a^2}, \quad \max_{\mathbf{x} \in \overline{\Omega}} \|\mathbf{B}(\mathbf{x})\| \le \frac{C_0}{a},
$$

where the number $C_0 = C_0(R, d) > 0$ depends only on the listed parameters. Hence, there exists a sufficiently large number $a_0 = a_0(N, R, d) > 1$ such that for any $a > a_0$ the matrix $\tilde{\mathbf{A}} = M_N(\mathrm{Id} - M_N^{-1}\mathbf{A})$ is invertible. Everywhere below we assume without further mentioning that $a > a_0$.

Denote $\mathbf{A}_1 := \tilde{\mathbf{A}}^{-1}\mathbf{B}$, $\mathbf{A}_2 := \tilde{\mathbf{A}}^{-1}\mathbf{C}$. Therefore, (3.7) is equivalent to

$$U_y - \mathbf{A}_1 U_x - \mathbf{A}_2 U = 0, \ \ \mathbf{A}_1 = \mathbf{A}_1(x,y), \ \ \mathbf{A}_2 = \mathbf{A}_2(x,y), \ \ (x,y) \in \Omega. \tag{3.11}$$

Using (2.8) and (2.9) we complement (3.11) with the following Dirichlet boundary condition:

$$U(\mathbf{x}) = F(\mathbf{x}) \ \text{ for } \ \mathbf{x} \in \partial\Omega, \tag{3.12}$$

where the vector function $F(\mathbf{x})$ is obtained from the function $Z(\mathbf{x},\alpha)$ in (2.8), (2.9) in the same way as the vector function $U(\mathbf{x})$ is obtained from the function $u(\mathbf{x},\alpha)$. Thus, we have obtained a system of coupled linear differential equations (3.11) with the boundary condition (3.12). The solution $U(\mathbf{x}) = (u_1(\mathbf{x}), \dots, u_N(\mathbf{x}))^T$ of the boundary value problem (3.11)–(3.12) directly yields the desired numerical solution to Problem 2.2 via the substitution of (3.2) in (2.3).

3.3. The QRM for problem (3.11)–(3.12). The problem (3.11)–(3.12) is an overdetermined one. Indeed, although (3.11) is of the first order, the boundary condition (3.12) is given on the entire boundary $\partial\Omega$. To find an approximate solution to this problem, we use the QRM, which, in general works properly for overdetermined problems for PDEs. Thus, we consider the following minimization problem for the Tikhonov-like functional J_ϵ with the regularization parameter $\epsilon \in (0,1)$:

$$J_\epsilon(U) = \int_\Omega |U_y - \mathbf{A}_1 U_x - \mathbf{A}_2 U|^2 dxdy + \epsilon \|U\|^2_{H^1(\Omega)}. \tag{3.13}$$

When we say below that a vector function belongs to a Hilbert space, we mean that each of its components belongs to this space and its norm is the square root of the sum of norms in that space of its components.

PROBLEM 3.1 (minimization problem). *Minimize the functional J_ϵ on the set of N-dimensional vector-valued functions $U \in H^1(\Omega)$ satisfying boundary condition* (3.12).

4. The fully discrete form of the QRM. To solve Problem 3.1, we write vector functions U_x, U_y in the functional $J_\epsilon(U)$ in finite differences and minimize this functional with respect to values of the vector function U at grid points. Hence, we formulate the QRM in this section in the fully discrete form of finite differences.

4.1. The fully discrete form of functional (3.13). Recall (2.1) and consider the following uniform 2D grid on $\overline{\Omega}$ whose x and y coordinates are given by

$$-R = x_0 < x_1 < \cdots < x_{M_x} = R, \ \ x_{i+1} - x_i = h_x \ \ \forall i \in \{0,1,\dots,M_x - 1\}, \tag{4.1}$$

$$a = y_0 < y_1 < \cdots < y_{M_y} = b, \ \ y_{j+1} - y_j = h_y \ \ \forall j \in \{0,1,\dots,M_y - 1\}. \tag{4.2}$$

Denote $h = (h_x, h_y)$. We define the discrete set Ω^h as

$$\begin{aligned}
\Omega^h &= \{(x,y) : \{(x_i,y_j)\}, i \in \{1,\dots,M_x - 1\}, \ \ j \in \{1,\dots,M_y - 1\}\},\\
\partial\Omega^h &= \{(x,y) : \{(x_i,y_j)\} \ \text{ for } \ i = 0,\dots,M_x, \ \ j = 0,\dots,M_y\},\\
\overline{\Omega}^h &= \Omega^h \cup \partial\Omega^h.
\end{aligned}$$

For any N-dimensional matrix $Q(x,y) \in C(\overline{\Omega})$ we introduce the following notations:

$$
\begin{aligned}
&\mathbf{Q}^h_{i,j} = Q(x_i, y_j),\ \ i \in \{1, \dots, M_x - 1\},\ \ j \in \{1, \dots, M_y - 1\},\\
&\widetilde{\mathbf{Q}}^h_{i,j} = Q(x_i, y_j),\ \ i \in \{0, \dots, M_x\},\ \ j \in \{0, \dots, M_y\},\\
&\mathbf{Q}^h \ = \left\{\mathbf{Q}^h_{i,j}\right\}_{i,j=1}^{M_x-1,M_y-1} \ \text{is an } (M_x-1)\times(M_y-1) \text{ matrix},\\
&\widetilde{\mathbf{Q}}^h \ = \left\{\mathbf{Q}^h_{i,j}\right\}_{i,j=0}^{M_x,M_y} \ \text{is an } (M_x+1)\times(M_y+1) \text{ matrix}.
\end{aligned} \tag{4.3}
$$

Note that the matrices $\mathbf{Q}^h$ and $\widetilde{\mathbf{Q}}^h$ coincide in Ω^h. However, unlike $\widetilde{\mathbf{Q}}^h$, the matrix $\mathbf{Q}^h$ does not include boundary terms of the form

$$
\mathbf{Q}^h_{0,j} = Q(-R, y_j),\ \ \mathbf{Q}^h_{i,0} = Q(x_i, a),\ \ \mathbf{Q}^h_{M_x,j} = Q(R, y_j),\ \ \mathbf{Q}^h_{i,M_y} = Q(x_i, b).
$$

Recall the forward finite difference formulas for the vector function $\mathbf{Q}^h$:

$$
(\mathbf{U}^h)'_x = \left\{(\mathbf{U}^h_{i,j})'_x\right\}_{i,j=0}^{M_x-1,M_y-1}, (\mathbf{U}^h_{i,j})'_x = \frac{\mathbf{U}^h_{i+1,j} - \mathbf{U}^h_{i,j}}{h_x},\ \ i \in \{0, \dots, M_x - 1\}, \tag{4.4}
$$

$$
(\mathbf{U}^h)'_y = \left\{(\mathbf{U}^h_{i,j})'_y\right\}_{i,j=0}^{M_x-1,M_y-1}, (\mathbf{U}^h_{i,j})'_y = \frac{\mathbf{U}^h_{i,j+1} - \mathbf{U}^h_{i,j}}{h_y},\ \ j \in \{0, \dots, M_y - 1\}. \tag{4.5}
$$

Hence, we obtain the following finite difference analog of (3.11)–(3.12):

$$
L^h\left(\mathbf{U}^h\right) = (\mathbf{U}^h)'_y - \mathbf{A}^h_1(\mathbf{U}^h)'_x + \mathbf{A}^h_2\mathbf{U}^h = 0;\ \ \mathbf{A}^h_1 = \mathbf{A}_1,\ \ \mathbf{A}^h_2 = \mathbf{A}_2 \ \text{ in } \Omega^h, \tag{4.6}
$$

$$
\widetilde{\mathbf{U}}^h = \mathbf{F}^h \ \text{ on } \partial\Omega^h, \tag{4.7}
$$

where the boundary matrix $\mathbf{F}^h$ is defined using the values of the vector function $F(\mathbf{x})$ in (3.12) on the grid (4.1), (4.2). We define discrete functional spaces of matrices Q^h, $\widetilde{\mathbf{Q}}^h$. These spaces $L^{2,h}(\Omega^h)$ and $H^{1,h}(\Omega^h)$ are discrete analogs of spaces $L^2(\Omega)$ and $H^1(\Omega)$, respectively. Norms in these analogs are defined as

$$
\|\mathbf{Q}^h\|_{L^{2,h}(\Omega^h)} = \left[h_y h_x \sum_{j=1}^{M_y-1}\sum_{i=1}^{M_x-1}\left(\mathbf{Q}^h_{i,j}\right)^2\right]^{1/2},
$$

$$
\|\widetilde{\mathbf{Q}}^h\|_{H^{1,h}(\Omega^h)} = \left[h_y h_x \sum_{i=1}^{M_x-1}\sum_{j=1}^{M_y-1}\left([(\mathbf{Q}^h_{i,j})'_x]^2 + [(\mathbf{Q}^h_{i,j})'_y]^2 + [\mathbf{Q}^h_{i,j}]^2\right)\right]^{1/2}.
$$

We define the inner products in these spaces in the obvious manner and denote them as $(\cdot,\cdot)$ and $[\cdot,\cdot]$ for $L^{2,h}(\Omega^h)$ and $H^{1,h}(\Omega^h)$, respectively. In addition, we define the subspace $H^{1,h}_0(\Omega^h)$ of the space $H^{1,h}(\Omega^h)$ as

$$
H^{1,h}_0(\Omega^h) = \left\{\widetilde{\mathbf{Q}}^h \in H^{1,h}(\Omega^h) : \widetilde{\mathbf{Q}}^h\ |_{\partial\Omega^h} = 0\right\}.
$$

Remark 4.1. Here and everywhere below if a matrix $\mathbf{Q}^h$ is defined as in (4.3), then $\widetilde{\mathbf{Q}}^h$ denotes the matrix $\mathbf{Q}^h$, complemented by boundary conditions at $\partial\Omega^h$.

Remark 4.2. Below we fix the number $h_1 \in (0,1)$ and restrict h_x from below as $h_x \in [h_1, 1)$. However, we do not restrict from below $h_y > 0$ by a positive constant.

Then it follows from (4.4) that there exists a constant $B_{h_1} > 0$ depending only on h_1 such that

$$\|(\mathbf{Q}^h)'_x\|^2_{L^{2,h}(\Omega^h)} \leq \quad B_{h_1}\|\mathbf{Q}^h\|^2_{L^{2,h}(\Omega^h)} \tag{4.8}$$

for all $\mathbf{Q}^h$ such that $\widetilde{\mathbf{Q}}^h \in H_0^{1,h}(\Omega^h)\ \forall h \in [h_1, 1]$.

Suppose that we have found the matrix $\mathbf{U}^h$. We now explain how to use backwards calculations to find the finite difference analog $f^h = (f(x_i, y_j))_{(i,j)=(1,1)}^{(M_x-1,M_y-1)}$ of the target function $f(\mathbf{x})$ of our ISOP. Recalling that by (3.7) and (4.3)

$$\mathbf{U}^h = \left(u_1^h, \dots, u_N^h\right)^T,\ u_n^h = \{u_n(x_i, y_j)\}_{(i,j)=(1,1)}^{(M_x-1,M_y-1)},\ n = 1, \dots, N, \tag{4.9}$$

and also recalling the original equation (2.3) as well as (2.6), (3.2), (4.3), and (4.5), we obtain for $i \in \{0, \dots, M_x - 1\}, j \in \{0, \dots, M_y - 1\}$,

$$\begin{aligned} f(x_i, y_j) = &\sum_{n=1}^{N} \Psi_n(\alpha) \left[\nu_1(x_i, y_j, \alpha)(u_n(x_i, y_j))_x + \nu_2(x_i, y_j, \alpha)(u_n(x_i, y_j))_y\right] \\ &+ (\mu_a(x_i, y_j) + \mu_s(x_i, y_j)) \sum_{n=1}^{N} \Psi_n(\alpha) u_n(x_i, y_j) \\ &- \mu_s(x_i, y_j) \int_{\Gamma_d} K(x_i, y_j, \alpha, \beta) \left(\sum_{n=1}^{N} \Psi_n(\beta) u_n(x_i, y_j)\right) d\beta. \end{aligned} \tag{4.10}$$

We assume that the right-hand side of (4.10) is independent of α. In practical computations we average the right-hand side of (4.10) over $\alpha \in (-d, d)$; see section 6.1.

Remark 4.3. By (4.3) here and everywhere below any matrix $\mathbf{Q}^h$ is defined only in interior points of $\overline{\Omega}^h$. On the other hand, $\widetilde{\mathbf{Q}}^h$ denotes the matrix $\mathbf{Q}^h$ complemented by boundary conditions at $\partial\Omega^h$.

The fully discrete QRM applied to problem (4.6)–(4.7) leads to the following discrete version of the above minimization problem.

PROBLEM 4.4 (discrete minimization problem). *Minimize the functional*

$$J_\epsilon^h(\widetilde{\mathbf{U}}^h) = \|(\mathbf{U}^h)'_y - \mathbf{A}_1^h(\mathbf{U}^h)'_x - \mathbf{A}_2^h\mathbf{U}^h\|^2_{L^{2,h}(\Omega^h)} + \epsilon\|\widetilde{\mathbf{U}}^h\|^2_{H^{1,h}(\Omega^h)} \tag{4.11}$$

on the set of matrices $\widetilde{\mathbf{U}}^h \in H^{1,h}(\Omega^h)$ *satisfying boundary condition* (4.7).

According to the theory of ill-posed problems [35], any minimizer of the functional $J_\epsilon^h(\widetilde{\mathbf{U}}^h)$ satisfying boundary condition (4.7) is called the *regularized solution* of the problem (4.6)–(4.7).

4.2. A discrete Carleman estimate. We now derive a discrete Carleman estimate for the finite difference version of the differential operator d/dy. Recalling (4.2), consider a uniform partition of the interval $(a, b) \subset \mathbb{R}$ of the real line into M subintervals with the grid step size h_y,

$$a = y_0 < y_1 < \cdots < y_M = b, \quad y_{j+1} - y_j = h_y, \quad j \in \{0, 1, \dots, M-1\}. \tag{4.12}$$

Following the book [32], for any discrete function u defined on this grid denote $u_j = u(y_j)$ and define both its forward u'_j and backward $\overline{u}'_j$ finite difference derivatives, which are the finite difference analogs of the differential operator d/dy, as

$$u'_j = \frac{(u_{j+1} - u_j)}{h_y}, j \in \{0, \dots, M-1\}, \quad \overline{u}'_j = \frac{(u_j - u_{j-1})}{h_y} \quad \forall j \in \{1, \dots, M\}. \tag{4.13}$$

LEMMA 4.5. *For any discrete function w, defined on the grid* (4.12), the following inequality holds:

$$-2h_y \sum_{j=1}^{M-1} w_j w'_j \geq -(w_M^2 - w_1^2).$$

Proof. Using the summation by parts formula for the discrete function w [32], we obtain

$$h_y \sum_{j=1}^{M-1} w_j w'_j = (w_M^2 - w_0 w_1) - h_y \sum_{i=1}^{M} w_i \overline{w_i}'.$$

Next,

$$\begin{aligned} h_y \sum_{i=1}^{M} w_i \overline{w_i}' &= h_y \sum_{j=0}^{M-1} w_{j+1} w'_j = h_y \sum_{j=0}^{M-1} (w_j + w'_j h_y) w'_j \\ &= h_y (w_0 + h w'_0) w'_0 + h_y \sum_{j=1}^{M-1} (w_j + w'_j h_y) w'_j \\ &= w_1 (w_1 - w_0) + h_y \sum_{j=1}^{M-1} (w_j + w'_j h_y) w'_j. \end{aligned}$$

Combining all equalities written above, we obtain

$$\begin{aligned} h_y \sum_{j=1}^{M-1} w_j w'_j &= \left(w_M^2 - w_0 w_1\right) - (w_1^2 - w_0 w_1) - h_y \sum_{j=1}^{M-1} \left(w_j + w'_j h_y\right) w'_j \\ &= \left(w_M^2 - w_1^2\right) - h_y \sum_{j=1}^{M-1} w_j w'_j - h_y^2 \sum_{j=1}^{M-1} (w'_j)^2. \end{aligned}$$

Hence,

$$-2h_y \sum_{j=1}^{M-1} w_j w'_j = -(w_M^2 - w_1^2) + h_y^2 \sum_{j=1}^{M-1} (w'_j)^2 \geq -\left(w_M^2 - w_1^2\right). \qquad \square$$

THEOREM 4.6 (a discrete Carleman estimate). *For any positive number $\lambda > 0$, the following discrete Carleman estimate holds for any discrete function u, defined on the grid* (4.12)*:*

$$\begin{aligned} h_y \sum_{j=1}^{M_y - 1} e^{2\lambda y_j} \left(u'_j\right)^2 \geq h_y \sum_{j=1}^{M_y - 1} &\left(\frac{1 - e^{-\lambda h_y}}{h_y}\right)^2 e^{2\lambda y_j} u_j^2 \\ &+ 2e^{-\lambda h_y} \left(\frac{1 - e^{-\lambda h_y}}{h_y}\right) (e^{2\lambda y_1} u_1^2 - e^{2\lambda y_M} u_M^2). \end{aligned}$$

Proof. For each j, we define

$$w_j = e^{\lambda y_j} u_j, \quad u_j = e^{-\lambda y_j} w_j. \tag{4.14}$$

Hence, according to (4.13), the forward difference derivative of the function u at y_j is

$$\begin{aligned} u_j' &= \frac{e^{-\lambda(y_j+h_y)} w_{j+1} - e^{-\lambda y_j} w_j}{h_y} = \frac{e^{-\lambda y_j}\left(e^{-\lambda h_y} w_{j+1} - w_j\right)}{h_y} \\ &= e^{-\lambda y_j}\left(e^{-\lambda h_y}\frac{w_{j+1}-w_j}{h_y} + \frac{e^{-\lambda h_y} w_j - w_j}{h_y}\right) \\ &= e^{-\lambda y_j}\left(w_j' e^{-\lambda h_y} - \frac{1-e^{-\lambda h_y}}{h_y} w_j\right). \end{aligned}$$

Hence, we have for each $j = 1, \dots, M_y - 1$,

$$\begin{aligned} e^{2\lambda y_j}(u_j')^2 &= \left(w_j' e^{-\lambda h_y} - \frac{1-e^{-\lambda h_y}}{h_y} w_j\right)^2 \\ &\geq \left(\frac{1-e^{-\lambda h_y}}{h_y}\right)^2 (w_j)^2 - 2e^{-\lambda h_y}\frac{\left(1-e^{-\lambda h_y}\right)}{h_y} w_j' w_j. \end{aligned}$$

As a result,

$$h_y \sum_{j=1}^{M_y-1} e^{2\lambda y_j}(u_j')^2 \geq h_y \sum_{j=1}^{M_y-1} \left(\frac{1-e^{-\lambda h_y}}{h_y}\right)^2 w_j^2 - 2e^{-\lambda h_y}\frac{(1-e^{-\lambda h_y})}{h_y} h_y \sum_{j=1}^{M-1} w_j' w_j.$$

Applying Lemma 4.5 to the second term on the right-hand side, we obtain

$$h_y \sum_{j=1}^{M_y-1} e^{2\lambda y_j}(u_j')^2 \geq h_y \sum_{j=1}^{M_y-1} \left(\frac{1-e^{-\lambda h_y}}{h_y}\right)^2 w_j^2 + \ 2e^{-\lambda h_y}\left(\frac{1-e^{-\lambda h_y}}{h_y}\right)(w_1^2 - w_M^2).$$

The statement of Theorem 4.6 follows from this estimate and (4.14). ∎

LEMMA 4.7. *Let u be a discrete function, defined on the grid* (4.12)*, such that $u_M = 0$. Then for any two numbers $\lambda, h_y > 0$ such that $\lambda h_y < 1$ the following inequality holds:*

$$h_y \sum_{j=1}^{M_y-1} e^{2\lambda y_j}\left(u_j'\right)^2 \geq \frac{\lambda^2}{4} h_y \sum_{j=1}^{M_y-1} e^{2\lambda y_j} u_j^2. \tag{4.15}$$

Proof. By the Taylor formula

$$e^{-\lambda h_y} = 1 - \lambda h_y + \frac{e^{-\xi}}{2}(\lambda h_y)^2 = 1 - \lambda h_y\left(1 - \frac{e^{-\xi}}{2}\lambda h_y\right),$$

where $\xi \in (0, \lambda h_y)$ is a certain number. Hence, $1 - e^{-\lambda h_y} \geq \lambda h_y/2$. Hence,

$$\left(\frac{1-e^{-\lambda h_y}}{h_y}\right)^2 \geq \frac{\lambda^2}{4}.$$

Therefore, using Theorem 4.6, we obtain (4.15). ∎

Remark 4.8. This lemma is a discrete analog of the Carleman estimate in [23, Lemma 4.1] for the continuous case of the operator d/dy.

5. Convergence analysis.

5.1. Existence of the solution of the discrete minimization problem. Let the matrix $\widetilde{\mathbf{G}}^h \in H^{1,h}(\Omega^h)$ be such that $\widetilde{\mathbf{G}}^h \mid_{\partial\Omega^h} = \mathbf{F}^h$. We need to work with the zero Dirichlet boundary condition at $\partial\Omega^h$. To do this, we introduce the matrix $\widetilde{\mathbf{W}}^h = \widetilde{\mathbf{U}}^h - \widetilde{\mathbf{G}}^h$. Hence, $\widetilde{\mathbf{W}}^h \in H_0^{1,h}(\Omega^h)$. Next, recalling notation (4.6) for the operator L^h, we rewrite the functional $J_\epsilon^h(\widetilde{\mathbf{U}}^h)$in the following form:

$$J_\epsilon^h(\widetilde{\mathbf{W}}^h) = \left\| L^h\left(\mathbf{W}^h\right) + L^h\left(\mathbf{G}^h\right)\right\|^2_{L^{2,h}(\Omega^h)} + \epsilon \left\|\widetilde{\mathbf{W}}^h + \widetilde{\mathbf{G}}^h\right\|^2_{H^{1,h}(\Omega^h)}, \tag{5.1}$$

$$\widetilde{\mathbf{W}}^h \in H_0^{1,h}(\Omega^h). \tag{5.2}$$

THEOREM 5.1. *For any $\epsilon > 0$ there exists unique minimizer $\widetilde{\mathbf{W}}^h_{\min,\epsilon} \in H_0^{1,h}(\Omega^h)$ of functional* (5.1). *Therefore, for any given matrix $\widetilde{\mathbf{G}}^h \in H^{1,h}(\Omega^h)$ satisfying the boundary condition $\widetilde{\mathbf{G}}^h \mid_{\partial\Omega^h} = \mathbf{F}^h$, there exists unique minimizer $\widetilde{\mathbf{U}}^h_{\min,\epsilon} = \widetilde{\mathbf{W}}^h_{\min,\epsilon} + \widetilde{\mathbf{G}}^h \in H^{1,h}(\Omega^h)$ of functional* (4.11) *satisfying boundary condition* (4.7).

Proof. Let $\widetilde{\mathbf{W}}^h_{\min,\epsilon}$ be any minimizer of functional (5.1) with condition (5.2). By the variational principle the following identity holds for all $\widetilde{\mathbf{P}}^h \in H_0^{1,h}(\Omega^h)$:

$$\begin{aligned}\left(L^h\left(\mathbf{W}^h_{\min,\epsilon}\right), L^h\left(\mathbf{P}^h\right)\right) + \epsilon\left[\widetilde{\mathbf{W}}^h_{\min,\epsilon}, \widetilde{\mathbf{P}}^h\right] \\ = -\left(L^h\left(\mathbf{G}^h\right), L^h\left(\mathbf{P}^h\right)\right) - \epsilon\left[\widetilde{\mathbf{G}}^h, \widetilde{\mathbf{P}}^h\right].\end{aligned} \tag{5.3}$$

The left-hand side of identity (5.3) generates a new scalar product $\{\cdot,\cdot\}$ in the subspace $H_0^{1,h}(\Omega^h)$. Consider the corresponding norm $\{\cdot\}^2$,

$$\left\{\widetilde{\mathbf{Q}}^h\right\}^2 = \left\|L^h\left(\mathbf{Q}^h\right)\right\|^2_{L^{2,h}(\Omega^h)} + \epsilon\left\|\mathbf{Q}^h\right\|^2_{H^{1,h}(\Omega^h)} \ \forall \widetilde{\mathbf{Q}}^h \in H_0^{1,h}(\Omega^h). \tag{5.4}$$

Obviously, there exists a certain constant $C_1 = C_1(L^h, h, \Omega^h, \epsilon) > 0$, which depends only on listed parameters such that

$$\epsilon\left\|\widetilde{\mathbf{Q}}^h\right\|^2_{H^{1,h}(\Omega^h)} \le \left\{\widetilde{\mathbf{Q}}^h\right\}^2 \le C_1\left\|\widetilde{\mathbf{Q}}^h\right\|^2_{H^{1,h}(\Omega^h)} \ \forall \widetilde{\mathbf{Q}}^h \in H_0^{1,h}(\Omega^h). \tag{5.5}$$

Below C_1 denotes different positive numbers depending on the same parameters.

Hence, norms $\{\widetilde{\mathbf{Q}}^h\}$ and $\|\widetilde{\mathbf{Q}}^h\|_{H^{1,h}(\Omega^h)}$ are equivalent for $\widetilde{\mathbf{Q}}^h \in H_0^{1,h}(\Omega^h)$. Therefore, (5.3) is equivalent to

$$\left\{\widetilde{\mathbf{W}}^h_{\min,\mu}, \widetilde{\mathbf{P}}^h\right\} = -\left(L^h\left(\mathbf{G}^h\right), L^h\left(\mathbf{P}^h\right)\right) - \epsilon\left[\widetilde{\mathbf{G}}^h, \widetilde{\mathbf{P}}^h\right] \ \forall \widetilde{\mathbf{P}}^h \in H_0^{1,h}(\Omega^h). \tag{5.6}$$

Using the Cauchy–Schwarz inequality, (5.4) and (5.5), we obtain

$$\left|-\left(L^h\left(\mathbf{G}^h\right), L^h\left(\mathbf{P}^h\right)\right) - \epsilon\left[\widetilde{\mathbf{G}}^h, \widetilde{\mathbf{P}}^h\right]\right| \le C_1\left\{\widetilde{\mathbf{G}}^h\right\}\left\{\widetilde{\mathbf{P}}^h\right\} \quad \forall \widetilde{\mathbf{P}}^h \in H_0^{1,h}(\Omega^h).$$

Hence, the right-hand side of (5.6) can be considered as a bounded linear functional acting on $\widetilde{\mathbf{P}}^h$ and mapping the space $H_0^{1,h}(\Omega^h)$ in $\mathbb{R}$. Since the regular norm in $H_0^{1,h}(\Omega^h)$ is equivalent to the norm generated by the new scalar product $\{\cdot,\cdot\}$, then the

Riesz representation theorem implies that there exists a unique matrix $\widetilde{\mathbf{\Phi}}^h \in H_0^{1,h}(\Omega^h)$ such that

$$\left\{\widetilde{\mathbf{W}}^h_{\min,\epsilon}, \widetilde{\mathbf{P}}^h\right\} = \left\{\widetilde{\mathbf{\Phi}}^h, \widetilde{\mathbf{P}}^h\right\} \quad \forall \widetilde{\mathbf{P}}^h \in H_0^{1,h}\left(\Omega^h\right).$$

Therefore, $\widetilde{\mathbf{W}}^h_{\min,\epsilon} = \widetilde{\mathbf{\Phi}}^h$. Finally, the matrix $\widetilde{\mathbf{U}}^h_{\min,\epsilon} = \widetilde{\mathbf{W}}^h_{\min,\epsilon} + \widetilde{\mathbf{G}}^h \in H^{1,h}(\Omega^h)$ is the unique minimizer claimed by this theorem. ∎

5.2. Convergence rate of regularized solutions, Lipschitz stability, and uniqueness. According to the regularization theory [35], the minimizer $\widetilde{\mathbf{U}}^h_{\min,\epsilon}$ is called the *regularized solution* . In this section, we establish the convergence rate of regularized solutions of problem (4.6)–(4.7) to the exact one when the level of noise in the data tends to zero. In addition, we establish a Lipschitz stability estimate and uniqueness for the problem (4.6)–(4.7).

Let a matrix $\mathbf{P}^h \in L^{2,h}(\Omega^h)$. Denote

$$\left\|\mathbf{P}^h e^{\lambda y}\right\|^2_{L^{2,h}(\Omega^h)} = h_y h_x \sum_{j=1}^{M_y-1} \sum_{i=1}^{M_x-1} \left(\mathbf{P}^h_{i,j}\right)^2 e^{2\lambda y_j}. \tag{5.7}$$

Hence, by Lemma 4.7 for all $\lambda > 0$ and for all h_y such that $\lambda h_y \in (0,1)$

$$\left\|\left(\mathbf{P}^h\right)'_y e^{\lambda y}\right\|^2_{L^{2,h}(\Omega^h)} \geq \frac{\lambda^2}{4} \left\|\mathbf{P}^h e^{\lambda y}\right\|^2_{L^{2,h}(\Omega^h)} \ \forall \widetilde{\mathbf{P}}^h \in H_0^{1,h}\left(\Omega^h\right). \tag{5.8}$$

Furthermore, by (4.8) for all $\lambda > 0, h_y > 0$, and for all $h_x \in [h_1, 1]$

$$\left\|\left(\mathbf{P}^h\right)'_x e^{\lambda y}\right\|^2_{L^{2,h}(\Omega^h)} \leq B_{h_1} \left\|\mathbf{P}^h e^{\lambda y}\right\|^2_{L^{2,h}(\Omega^h)} \ \forall \widetilde{\mathbf{P}}^h \in H_0^{1,h}\left(\Omega^h\right). \tag{5.9}$$

LEMMA 5.2. *There exist a sufficiently small number $h_y^0 = h_y^0(N, d, R, h_1, a, b, L^h)$ in $(0,1)$ and a number $C_2 = C_2(N, d, R, h_1, h_y^0, a, b, L^h) > 0$, both depending only on listed parameters, such that for $h_x \in [h_1, 1), h_y \in (0, h_y^0]$ the following estimate is valid:*

$$\left\|L^h\left(\mathbf{Q}^h\right)\right\|^2_{L^{2,h}(\Omega^h)} \geq C_2 \left\|\mathbf{Q}^h\right\|^2_{L^{2,h}(\Omega^h)}, \quad \forall \widetilde{\mathbf{Q}}^h \in H_0^{1,h}(\Omega^h). \tag{5.10}$$

Remark 5.3. Everywhere below $C_2 > 0$ denotes different constants depending only on the above listed parameters.

Proof of Lemma 5.2. Using the definition of the operator L^h in (4.6) as well as (5.9) and the Cauchy–Schwarz inequality, we obtain

$$\begin{aligned} \left\|L^h\left(\mathbf{Q}^h\right)\right\|^2_{L^{2,h}(\Omega^h)} &= \left\|L^h\left(\mathbf{Q}^h\right) e^{\lambda y} e^{-\lambda y}\right\|^2_{L^{2,h}(\Omega^h)} \geq e^{-2\lambda b} \left\|L^h\left(\mathbf{Q}^h\right) e^{\lambda y}\right\|^2_{L^{2,h}(\Omega^h)} \\ &\geq \frac{1}{2} e^{-2\lambda b} \left[\left\|\left(\mathbf{Q}^h\right)'_y e^{\lambda y}\right\|^2_{L^{2,h}(\Omega^h)} - C_2 \left\|\mathbf{Q}^h e^{\lambda y}\right\|^2_{L^{2,h}(\Omega^h)}\right]. \end{aligned} \tag{5.11}$$

Choose $h_y^0 \in (0,1)$ so small that $1/(h_y^0)^2 > 32C_2$. Let $h_y \in (0, h_y^0)$. Set $\lambda = 1/(2h_y^0)$. Then $\lambda h_y < \lambda h_y^0 = 1/2 < 1$ and also $\lambda^2/4 = 1/(16(h_y^0)^2) > 2C_2$. Hence, using (5.8)

and (5.11), we obtain

$$\begin{aligned}\left\|L^h\left(\mathbf{Q}^h\right)\right\|^2_{L^{2,h}(\Omega^h)} &\geq \frac{1}{2}e^{-2\lambda b}\left[\frac{\lambda^2}{4}\left\|\mathbf{Q}^h e^{\lambda y}\right\|^2_{L^{2,h}(\Omega^h)} - C_2\left\|\mathbf{Q}^h e^{\lambda y}\right\|^2_{L^{2,h}(\Omega^h)}\right]\\ &\geq \frac{1}{2}e^{-2\lambda b}\left(2C_2\left\|\mathbf{Q}^h e^{\lambda y}\right\|^2_{L^{2,h}(\Omega^h)} - C_2\left\|\mathbf{Q}^h e^{\lambda y}\right\|^2_{L^{2,h}(\Omega^h)}\right)\\ &= \frac{1}{2}e^{-2\lambda b}C_2\left\|\mathbf{Q}^h e^{\lambda y}\right\|^2_{L^{2,h}(\Omega^h)}.\end{aligned}$$

This estimate immediately implies (5.10) with a new constant $C_2 > 0$. ∎

According to the theory of ill-posed problems [35], we assume that there exists a solution $\widetilde{\mathbf{U}}^{*h} \in H^{1,h}(\Omega^h)$ of problem (4.6)–(4.7) with the noiseless boundary data $\mathbf{F}^{*,h}$. This solution is unique; see Theorem 5.5. Let the matrix $\widetilde{\mathbf{G}}^{*,h}$ be such that

$$\widetilde{\mathbf{G}}^{*,h} \in H^{1,h}(\Omega^h),\ \widetilde{\mathbf{G}}^{*,h}\mid_{\partial\Omega^h} = \mathbf{F}^{*,h}.$$

Consider the boundary data $\mathbf{F}^h$ with a noise of the level $\delta \in (0,1)$. More precisely, we assume that there exists a matrix $\widetilde{\mathbf{G}}^h \in H^{1,h}(\Omega^h)$ such that $\widetilde{\mathbf{G}}^h\mid_{\partial\Omega^h} = \mathbf{F}^h$ and also

$$\|\widetilde{\mathbf{G}}^{*,h} - \widetilde{\mathbf{G}}^h\|_{H^{1,h}(\Omega^h)} \leq \delta. \tag{5.12}$$

As it is often the case in the regularization theory, it is convenient to indicate the dependence of the minimizer $\mathbf{U}^h_{\min,\epsilon}$ on the noise level δ. Thus, we denote $\mathbf{U}^h_{\min,\epsilon}$ as $\mathbf{U}^h_{\min,\epsilon,\delta}$.

THEOREM 5.4 (convergence rate of regularized solutions). *Assume that condition* (5.12) *holds. Let* $\mathbf{U}^h_{\min,\epsilon,\delta} \in H^{1,h}(\Omega^h)$ *be the unique minimizer of the functional* (4.11) *that satisfies boundary condition* (4.7) *(see Theorem* 5.1*). Suppose that* $\epsilon \in (0,1)$, $h_x \in [h_1, 1)$, *and* $h_y \in (0, h_y^0]$, *where the number* h_y^0 *is defined in Lemma* 5.2. *Then the following convergence rate of regularized solutions holds:*

$$\|\mathbf{U}^h_{\min,\epsilon,\delta} - \mathbf{U}^{*h}\|_{L^{2,h}(\Omega^h)} \leq C_2(\delta + \sqrt{\epsilon}\|\widetilde{\mathbf{U}}^{*h}\|_{H^{1,h}(\Omega^h)}). \tag{5.13}$$

Proof. As to the constant C_2, see Remark 5.3. Define matrices $\widetilde{\mathbf{W}}^{*,h}, \widetilde{\mathbf{W}}^h_{\min,\epsilon,\delta} \in H^{1,h}_0(\Omega^h)$ as

$$\widetilde{\mathbf{W}}^{*,h} = \widetilde{\mathbf{U}}^{*,h} - \widetilde{\mathbf{G}}^{*,h},\ \widetilde{\mathbf{W}}^h_{\min,\epsilon,\delta} = \widetilde{\mathbf{U}}^h_{\min,\epsilon,\delta} - \widetilde{\mathbf{G}}^h. \tag{5.14}$$

Then the identity (5.3) is valid for $\mathbf{W}^h_{\min,\epsilon,\delta}$. By (4.6) $L^h(\mathbf{W}^{*,h} + \mathbf{G}^{*,h}) = 0$. Hence,

$$\begin{aligned}&\left(L^h\left(\mathbf{W}^{*,h} + \mathbf{G}^{*,h}\right), L^h\left(\mathbf{P}^h\right)\right) + \epsilon\left[\widetilde{\mathbf{W}}^{*,h} + \widetilde{\mathbf{G}}^{*,h}, \widetilde{\mathbf{P}}^h\right]\\ &\qquad = \epsilon\left[\widetilde{\mathbf{W}}^{*,h} + \widetilde{\mathbf{G}}^{*,h}, \widetilde{\mathbf{P}}^h\right]\end{aligned} \tag{5.15}$$

for all $\widetilde{\mathbf{P}}^h \in H^{1,h}_0(\Omega^h)$. Denote

$$\widetilde{\mathbf{V}}^h_{\min,\epsilon,\delta} = \widetilde{\mathbf{W}}^h_{\min,\epsilon,\delta} - \widetilde{\mathbf{W}}^{*,h} \in H^{1,h}_0(\Omega^h). \tag{5.16}$$

Next, subtract (5.15) from (5.3). We obtain

$$\begin{aligned}&\left(L^h\left(\mathbf{V}^h_{\min,\epsilon,\delta}\right), L^h\left(\mathbf{P}^h\right)\right) + \epsilon\left[\widetilde{\mathbf{V}}^h_{\min,\epsilon,\delta}, \widetilde{\mathbf{P}}^h\right]\\ &\quad = -\left(L^h\left(\mathbf{G}^h - \mathbf{G}^{*,h}\right), L^h\left(\mathbf{P}^h\right)\right) - \epsilon\left[\widetilde{\mathbf{W}}^{*,h} + \widetilde{\mathbf{G}}^h, \widetilde{\mathbf{P}}^h\right]\ \forall \widetilde{\mathbf{P}}^h \in H^{1,h}_0(\Omega^h).\end{aligned} \tag{5.17}$$

Set in (5.17) $\widetilde{\mathbf{P}}^h = \widetilde{\mathbf{V}}^h_{\min,\epsilon,\delta}$, use the Cauchy–Schwarz inequality as well as (5.12). We obtain

$$\begin{aligned}\left\|L^h\left(\mathbf{V}^h_{\min,\epsilon,\delta}\right)\right\|^2_{L^{2,h}(\Omega^h)} &\le \left\|L^h\left(\mathbf{G}^h-\mathbf{G}^{*,h}\right)\right\|^2_{L^{2,h}(\Omega^h)} + \epsilon\left\|\widetilde{\mathbf{W}}^{*,h}+\widetilde{\mathbf{G}}^h\right\|^2_{H^{1,h}(\Omega^h)}\\ &\le C_2\delta^2 + \epsilon\left\|\widetilde{\mathbf{W}}^{*,h}+\widetilde{\mathbf{G}}^h\right\|^2_{H^{1,h}(\Omega^h)}. \qquad (5.18)\end{aligned}$$

Next, using (5.10) and (5.18), we obtain

$$\left\|\mathbf{V}^h_{\min,\epsilon,\delta}\right\|^2_{L^{2,h}(\Omega^h)} \le C_2\left(\delta^2+\epsilon\left\|\widetilde{\mathbf{W}}^{*,h}+\widetilde{\mathbf{G}}^h\right\|^2_{H^{1,h}(\Omega^h)}\right).$$

Hence,

$$\left\|\mathbf{V}^h_{\min,\epsilon,\delta}\right\|_{L^{2,h}(\Omega^h)} \le C_2\left(\delta+\sqrt{\epsilon}\left\|\widetilde{\mathbf{W}}^{*,h}+\widetilde{\mathbf{G}}^h\right\|_{H^{1,h}(\Omega^h)}\right). \qquad (5.19)$$

Using the triangle inequality, (5.12), and (5.14), we obtain

$$\begin{aligned}\left\|\widetilde{\mathbf{W}}^{*,h}+\widetilde{\mathbf{G}}^h\right\|_{H^{1,h}(\Omega^h)} &= \left\|\left(\widetilde{\mathbf{W}}^{*,h}+\widetilde{\mathbf{G}}^{*,h}\right)+\left(\widetilde{\mathbf{G}}^h-\widetilde{\mathbf{G}}^{*,h}\right)\right\|_{H^{1,h}(\Omega^h)}\\ &\le \left\|\widetilde{\mathbf{W}}^{*,h}+\widetilde{\mathbf{G}}^{*,h}\right\|_{H^{1,h}(\Omega^h)} + \left\|\widetilde{\mathbf{G}}^h-\widetilde{\mathbf{G}}^{*,h}\right\|_{H^{1,h}(\Omega^h)} \qquad (5.20)\\ &\le \left\|\widetilde{\mathbf{U}}^{*,h}\right\|_{H^{1,h}(\Omega^h)}+\delta.\end{aligned}$$

Since $\epsilon\in(0,1)$, then (5.19) and (5.20) imply

$$\left\|\mathbf{V}^h_{\min,\epsilon,\delta}\right\|_{L^{2,h}(\Omega^h)} \le C_2\left(\delta+\sqrt{\epsilon}\left\|\widetilde{\mathbf{U}}^{*,h}\right\|_{H^{1,h}(\Omega^h)}\right). \qquad (5.21)$$

Next, using (5.12), (5.14), (5.16), (5.21), and the triangle inequality, we obtain

$$\begin{aligned}\|\mathbf{U}^h_{\min,\epsilon,\delta}-\mathbf{U}^{*h}\|_{L^{2,h}(\Omega^h)} &= \|\left(\mathbf{W}^h_{\min,\epsilon,\delta}+\mathbf{G}^h\right)-\left(\mathbf{W}^{*,h}+\mathbf{G}^{*,h}\right)\|_{L^{2,h}(\Omega^h)}\\ &= \left\|\mathbf{V}^h_{\min,\epsilon,\delta}+\left(\mathbf{G}^h-\mathbf{G}^{*,h}\right)\right\|_{L^{2,h}(\Omega^h)}\\ &\le \left\|\mathbf{V}^h_{\min,\epsilon,\delta}\right\|_{L^{2,h}(\Omega^h)}+\left\|\widetilde{\mathbf{G}}^h-\widetilde{\mathbf{G}}^{*,h}\right\|_{L^{2,h}(\Omega^h)}.\end{aligned}$$

Using this estimate, (5.12), and (5.21), we obtain

$$\|\mathbf{U}^h_{\min,\epsilon,\delta}-\mathbf{U}^{*h}\|_{L^{2,h}(\Omega^h)} \le C_2\left(\delta+\sqrt{\epsilon}\left\|\widetilde{\mathbf{U}}^{*,h}\right\|_{H^{1,h}(\Omega^h)}\right)+\delta. \qquad (5.22)$$

The target estimate (5.13) follows from (5.22) with a new constant C_2. ∎

THEOREM 5.5 (Lipschitz stability and uniqueness). *Let two matrices $\mathbf{G}^h_1,\mathbf{G}^h_2\in H^{1,h}(\Omega^h)$ be such that $\widetilde{\mathbf{G}}^h_1\,|_{\partial\Omega^h}=\mathbf{F}^h_1$ and $\widetilde{\mathbf{G}}^h_2\,|_{\partial\Omega^h}=\mathbf{F}^h_2$, where $\mathbf{F}^h_1$ and $\mathbf{F}^h_2$ are two different boundary conditions in* (4.7). *Suppose that there exist solutions $\widetilde{\mathbf{U}}^h_1\in H^{1,h}(\Omega^h)$ and $\widetilde{\mathbf{U}}^h_2\in H^{1,h}(\Omega^h)$ of boundary value problem* (4.6)–(4.7) *with boundary conditions $\mathbf{F}^h_1$ and $\mathbf{F}^h_2$, respectively. Assume that $h_x\in[h_1,1)$ and $h_y\in(0,h^0_y]$, where the number h^0_y is defined in Lemma* 5.2. *Then the following Lipschitz stability estimate is valid:*

$$\left\|\mathbf{U}^h_1-\mathbf{U}^h_2\right\|_{L^{2,h}(\Omega^h)} \le C_2\left\|\mathbf{G}^h_1-\mathbf{G}^h_2\right\|_{L^{2,h}(\Omega^h)}. \qquad (5.23)$$

Next, suppose that $\mathbf{F}^h_1=\mathbf{F}^h_2$. Then $\mathbf{U}^h_1=\mathbf{U}^h_2$ in Ω^h, where $\mathbf{U}^h_1,\mathbf{U}^h_2\in H^{1,h}(\Omega^h)$ are two possible solutions of boundary value problem (4.6)–(4.7).

Proof. See Remark 5.3 about the constant C_2. Since $\widetilde{\mathbf{U}}_1^h$ and $\widetilde{\mathbf{U}}_2^h$ are two exact solutions of problem (4.6)–(4.7) with two different boundary conditions, then by (4.6)

$$\left(L^h\left(\mathbf{W}_i^h\right), L^h\left(\mathbf{P}^h\right)\right) = -\left(L^h\left(\mathbf{G}_i^h\right), L^h\left(\mathbf{P}^h\right)\right) \ \forall \mathbf{P}^h \in H_0^{1,h}\left(\Omega^h\right), i = 1, 2, \tag{5.24}$$

where $\widetilde{\mathbf{W}}_i^h = \widetilde{\mathbf{U}}_i^h - \widetilde{\mathbf{G}}_i^h$. Setting $\mathbf{S}^h = \mathbf{W}_1^h - \mathbf{W}_2^h, \mathbf{X}^h = \mathbf{G}_1^h - \mathbf{G}_2^h$ and then setting $\mathbf{P}^h = \mathbf{S}^h$, we obtain from (5.24) and (4.8)

$$\left\|L^h\left(\mathbf{S}^h\right)\right\|^2_{L^{2,h}(\Omega^h)} \leq \left\|L^h\left(\mathbf{X}^h\right)\right\|^2_{L^{2,h}(\Omega^h)} \leq C_2 \left\|\mathbf{X}^h\right\|^2_{L^{2,h}(\Omega^h)}.$$

Hence, by (5.10) $\|\mathbf{S}^h\|^2_{L^{2,h}(\Omega^h)} \leq C_2 \|\mathbf{X}^h\|^2_{L^{2,h}(\Omega^h)}$. Therefore,

$$\left\|\left(\mathbf{U}_1^h - \mathbf{U}_2^h\right) - \left(\mathbf{G}_1^h - \mathbf{G}_2^h\right)\right\|_{L^{2,h}(\Omega^h)} \leq C_2 \left\|\mathbf{G}_1^h - \mathbf{G}_2^h\right\|_{L^{2,h}(\Omega^h)}. \tag{5.25}$$

Thus, (5.23) follows from (5.25) and the triangle inequality.

As to the uniqueness part, since $\mathbf{F}_1^h = \mathbf{F}_2^h$, then we extend the boundary condition $\mathbf{F}_1^h - \mathbf{F}_2^h = \widehat{\mathbf{F}}^h = 0$ in the domain Ω^h as $\mathbf{G}_1^h - \mathbf{G}_2^h = \widehat{\mathbf{G}}^h = 0$. Hence, (5.23) implies that

$$\mathbf{U}_1^h - \mathbf{U}_2^h = 0 \text{ in } \Omega^h. \tag{5.26}$$ ∎

The next theorem is about uniqueness of the original ISOP within the framework of our approximate mathematical model; see Remarks 4.3 and 5.7 about this model. Although a direct analog of the Lipshitz stability estimate (5.23) also holds in this case, we do not formulate it for brevity.

THEOREM 5.6 (uniqueness of the ISOP). *In terms of Theorem* 5.5*, assume again that* $\mathbf{F}_1^h = \mathbf{F}_2^h$*. Let* f_1^h *and* f_2^h *be two such functions* f^h*, whose values at grid points of* Ω^h *are defined in* (4.10)*. Then*

$$f_1^h = f_2^h. \tag{5.27}$$

Proof. Just as in the end of the proof of Theorem 5.5, extend the boundary data $\mathbf{F}_1^h - \mathbf{F}_2^h = \widehat{\mathbf{F}}^h = 0$ inside the domain Ω^h as $\mathbf{G}_1^h - \mathbf{G}_2^h = \widehat{\mathbf{G}}^h = 0$. Then we obtain (5.26). Next, (4.9) and (4.10) imply (5.27). ∎

Remark 5.7. Suppose that there exists a solution of the original ISOP 2.2 with noiseless data (2.8) with condition (2.9). Suppose also that this solution is unique. Due to the ill-posedness of Problem 2.2, we cannot prove convergence of our solutions to that one as $N \to \infty$ and $M_x \to \infty$. At the same time, we can prove convergence as $M_y \to \infty$ since one of conditions of Lemma 4.3 is $h_y \in (0, 1/\lambda)$. We note that the truncated Fourier series are used both quite often and quite successfully in numerical methods for many inverse problems. Although convergence at $N \to \infty$ is not proven in many cases, numerical results are usually good ones; see, e.g., [10] for the attenuated tomography with complete data, [14] for the 2D version of the Gel'fand–Levitan method, [26] for the inverse problem of finding initial condition of heat equation, [30] for the ISOP for the Helmholtz equation, and [18, 21, 22] for the globally convergent numerical methods for CIPs mentioned in section 1.

6. Numerical implementation. In this section, we describe the numerical implementation of the minimization procedure for the functional J_ϵ^h. While inverting

the matrix M_N of (3.7) is convenient for the convergence analysis, we have discovered that it is better in real computations not to invert this matrix while still to consider a problem which is equivalent to the problem (4.6)–(4.7). Thus, we consider the functional (4.11) in a slightly different form:

$$J^h_{\epsilon_1,\epsilon_2}(\widetilde{\mathbf{U}}^h) = \|(M_N - \mathbf{A}^h)(\mathbf{U}^h)'_y - \mathbf{B}^h(\mathbf{U}^h)'_x - \mathbf{C}^h\mathbf{U}^h\|^2_{L^{2,h}(\Omega^h)} + \epsilon_1\|\mathbf{U}^h\|^2_{L^{2,h}(\Omega^h)} + \epsilon_2\|\nabla\mathbf{U}^h\|^2_{L^{2,h}(\Omega^h)},$$

where $\mathbf{A}^h, \mathbf{B}^h, \mathbf{C}^h$ are operators (3.8)–(3.10), with the domain $\overline{\Omega}_h$. Moreover, in contrast to the original functional, we use in our computations two regularization parameters ϵ_1 and ϵ_2, instead of just one parameter ϵ. This yields better reconstruction results. The regularization parameters ϵ_1, ϵ_2 in our numerical tests were found by a trial and error procedure. They were the same for all the tests we have conducted.

To minimize the functional $J^h_{\epsilon_1,\epsilon_2}(\widetilde{\mathbf{U}}^h)$, we first have to simulate the boundary data via solving Problem 2.1. We discuss the solution of this forward problem in appendix. Using this solution, we generate the noisy data as (see (2.8), (2.9), and (5.12))

$$Z(\mathbf{x},\alpha) = \begin{cases} u^{comp}_\delta(\mathbf{x},\alpha) = u^{comp}(\mathbf{x},\alpha)(1+\delta(2\mathrm{rand}(\mathbf{x})-1)), & \mathbf{x}\in\partial\Omega\setminus\partial\Omega^+, \\ 0, & \mathbf{x}\in\partial\Omega^+, \end{cases}$$

where $u^{comp}(\mathbf{x},\alpha)$ is the boundary data computed via the solution of the forward problem, $\delta > 0$ is the noise level, and $\mathrm{rand}(\cdot)$ is the function that generates uniformly distributed random numbers in the interval $[0,1]$. For example, $\delta = 0.6$ corresponds to the 60% noise level in the data.

We use the finite difference approximations (4.4), (4.5) on the grid with $h_x = h_y$, $M_x = M_y$. We rewrite the functional $J^h_{\epsilon_1,\epsilon_2}$ in the following discrete form:

$$\begin{aligned} &J^h_{\epsilon_1,\epsilon_2}(\widetilde{\mathbf{U}}^h) \\ &= h_{\mathbf{x}}^2\sum_{i,j=1}^{M_x-1}\left((M_N-\mathbf{A}^h)_{ij}\frac{\mathbf{U}^h_{i,j+1}-\mathbf{U}^h_{i,j}}{h_x} - (\mathbf{B}^h)_{ij}\frac{\mathbf{U}^h_{i+1,j}-\mathbf{U}^h_{i,j}}{h_x} - (\mathbf{C}^h)_{ij}\mathbf{U}^h_{i,j}\right)^2 \\ &\quad + \epsilon_1 h_x^2\sum_{i,j=1}^{M_x-1}\left(\mathbf{U}^h_{i,j}\right)^2 + \epsilon_2 h_x^2\sum_{i,j=1}^{M_x-1}\left(\frac{|\mathbf{U}^h_{i,j+1}-\mathbf{U}^h_{i,j}|^2}{h_x} + \frac{|\mathbf{U}^h_{i+1,j}-\mathbf{U}^h_{i,j}|^2}{h_x}\right). \end{aligned}$$

Denote $u_m(x_i,y_j) = u^{i,j}_m$. Since $\mathbf{U} := (u_1(x,y),\dots,u_N(x,y))^T$, then

$$\begin{aligned} &J^h_{\epsilon_1,\epsilon_2}(\widetilde{\mathbf{U}}^h) \\ &= h_x^2\sum_{i,j=1}^{M_x-1}\sum_{m=1}^{N}\left((M_N-\mathbf{A}^h)_{ij}\frac{u^{i,j+1}_m-u^{i,j}_m}{h_x} - (\mathbf{B}^h)_{ij}\frac{u^{i+1,j}_m-u^{i,j}_m}{h_x} - (\mathbf{C}^h)_{ij}u^{i,j}_m\right)^2 \\ &\quad + \epsilon_1 h_x^2\sum_{i,j=1}^{M_x-1}\sum_{m=1}^{N}\left(u^{i,j}_m\right)^2 + \epsilon_2 h_x^2\sum_{i,j=1}^{M_x-1}\sum_{m=1}^{N}\left(\frac{|u^{i,j+1}_m-u^{i,j}_m|^2}{h_x} + \frac{|u^{i+1,j}_m-u^{i,j}_m|^2}{h_x}\right). \end{aligned}$$

Introduce the "lined-up" versions of the matrices $\widetilde{\mathbf{U}}^h, M_N - \mathbf{A}^h, \mathbf{B}^h, \mathbf{C}^h$. The $(M_x+1)^2N$-dimensional vector $\mathcal{U}$,

$$\mathcal{U}_{\mathfrak{m}} = u_m(x_i,y_j), \quad 1\le i,j\le M_x+1, 1\le m\le N, \tag{6.1}$$

and the $(M_x+1)^2N\times(M_x+1)^2N$-dimensional matrices $\mathcal{A}^h, \mathcal{B}^h, \mathcal{C}^h$, corresponding

to $M_N - \mathbf{A}^h, \mathbf{B}^h, \mathbf{C}^h$, where

$$\mathfrak{m} = (i-1)(M_x+1)N + (j-1)N + m. \tag{6.2}$$

We introduce the map

$$\{1,\dots,M_x+1\} \times \{1,\dots,M_x+1\} \times \{1,\dots,N\} \to \{1,\dots,(M_x+1)^2 N\}$$

that sends (i,j,m) to $\mathfrak{m}$ as in (6.2), is onto, and one-to-one. The functional $J^h_{\epsilon_1,\epsilon_2}(\widetilde{\mathbf{U}}^h)$ is rewritten in terms of the lined-up vector $\mathcal{U}$ as

$$\mathcal{J}^h_{\epsilon_1,\epsilon_2}(\mathcal{U}) = h_x^2 \left(|\mathcal{L}\mathcal{U}|^2 + \epsilon_1 |\mathcal{U}|^2 + \epsilon_2 |\mathcal{D}_x \mathcal{U}|^2 + \epsilon_2 |\mathcal{D}_y \mathcal{U}|^2 \right), \tag{6.3}$$

where $\mathcal{D}_x$ and $\mathcal{D}_y$ are the matrices that provide the finite difference analogs of the partial derivatives of $\mathcal{U}$ with respect to x and y, defined similarly to (4.4), (4.5). $\mathcal{L}$ is the $(M_x+1)^2 N \times (M_x+1)^2 N$ matrix defined as follows. For each

$$\mathfrak{m} = (i-1)(M_x+1)N + (j-1)N + m, 2 \le i,j \le M_x, 1 \le m \le N, \tag{6.4}$$

1. $\mathcal{L}_{\mathfrak{m}\mathfrak{n}} = (-(\mathcal{A}^h)_{\mathfrak{m}\mathfrak{n}} + (\mathcal{B}^h)_{\mathfrak{m}\mathfrak{n}})/h_x - (\mathcal{C}^h)_{\mathfrak{m}\mathfrak{n}}$ if $\mathfrak{m}$ corresponds to (i,j,n) in the sense of (6.4) for each $n \in \{1,\dots,N\}$;
2. $\mathcal{L}_{\mathfrak{m}\mathfrak{n}} = (\mathcal{A}^h)_{\mathfrak{m}\mathfrak{n}}/h_x$ if $\mathfrak{m}$ corresponds to $(i,j+1,n)$ in the sense of (6.4) for each $n \in \{1,\dots,N\}$;
3. $\mathcal{L}_{\mathfrak{m}\mathfrak{n}} = -(\mathcal{B}^h)_{\mathfrak{m}\mathfrak{n}}/h_x$ if $\mathfrak{m}$ corresponds to $(i+1,j,n)$ in the sense of (6.4) for each $n \in \{1,\dots,N\}$;
4. $\mathcal{L}_{\mathfrak{m}\mathfrak{n}} = 0$ otherwise.

Next, we consider the lined-up version of the boundary condition (4.7). Let $\mathcal{D}$ be the $(M_x+1)^2 N \times (M_x+1)^2 N$ diagonal matrix with $\mathfrak{m}$th diagonal entries taking value 1 while the others equal 0. This Dirichlet boundary constraint of the vector $\mathcal{U}$ becomes $\mathcal{D}\mathcal{U} = \tilde{\mathcal{F}}$. Here, the vector $\tilde{\mathcal{F}}$ is the lined-up vector of the data F_N in the same manner as when we defined $\mathcal{U}$; see (6.1). We solve the ISOP by computing the vector $\mathcal{U}$, subject to constraint $\mathcal{D}\mathcal{U} = \tilde{\mathcal{F}}$, such that

$$\mathcal{L}_\mu \mathcal{U} = \left(\mathcal{L}^T \mathcal{L} + \epsilon_1 \mathrm{Id} + \epsilon_2 \mathcal{D}_x^T \mathcal{D}_x + \epsilon_2 \mathcal{D}_y^T \mathcal{D}_y \right) \mathcal{U} = \vec{0}, \tag{6.5}$$

which is equivalent to the minimization of the functional (6.3).

The knowledge of $\mathcal{U}$ yields the knowledge of $\widetilde{\mathbf{U}}^h$ via (6.1). Denote the result obtained by the procedure of this section as $\widetilde{\mathbf{U}}^{comp} = (u_1^{comp}(x,y), \dots, u_N^{comp}(x,y))^T$. Using this matrix, we calculate the function $u^{comp}(x,y,\alpha)$ via (3.2). Consider a grid point (x_i, y_j), where $i \in \{0,\dots,M_x-1\}, j \in \{0,\dots,M_y-1\}$. Then the reconstructed function $f^{comp}(x_i,y_j)$ is determined as the averaged value over $\alpha \in (-d,d)$ of the source function $f^{comp}(x_i,y_j,\alpha)$ calculated via the substitution of $u^{comp}(x_i,y_j,\alpha)$ in (4.10).

These arguments lead to Algorithm 6.1 for solving Problem 2.2.

6.1. Numerical tests. We test our method using numerical simulations for different types of absorption and scattering coefficients. Test 1 demonstrates the stability of the solution in the "no scattering" model, which corresponds to the $\mu_s(\mathbf{x},\alpha) \equiv 0$ value of the scattering coefficient. Moreover, Test 1 is used to find the optimal parameters, $\epsilon_1, \epsilon_2, d, N$, which we use in subsequent tests. The optimal values for those listed parameters are $\epsilon_1 = 0.1, \epsilon_2 = 0.01, d = 5, N = 12$.

In Test 2 we consider the "uniform scattering" version of the RTE for the object with a nonsmooth boundary, where $\mu_s(\mathbf{x}) \not\equiv 0, K(\mathbf{x},\alpha,\beta) = 1/(2d)$.

Algorithm 6.1 The procedure to solve Problem 2.2.

1: Choose a number N. Construct the functions Ψ_m, $1 \le m \le N$, in section 3.1 and compute the matrix M_N as in (3.1).
2: Calculate the boundary data $\mathbf{F}^h$ for the vector-valued function $\widetilde{\mathbf{U}}^h$ on $\partial\Omega^h$ via solving Problem 2.1 with $f = f_{true}$.
3: Find an approximate solution of (4.6)–(4.7) by the QRM.
4: Having $\widetilde{\mathbf{U}}^h$, calculate $u_{comp}(\mathbf{x}, \alpha)$ for $\mathbf{x} \in \Omega^h$ via (3.2).
5: Compute the reconstructed function f_{comp} by (2.3).

Test 3 demonstrates the performance of our method for both the sophisticated form of the absorption coefficient $\mu_a(\mathbf{x})$ and the "strongly forward-peaked scattering" case, i.e., the case when the scattered particles move in the direction preferentially close to the one they were moving. That corresponds to the case when $\mu_s(\mathbf{x}) \not\equiv 0$ and $K(\mathbf{x}, \alpha, \beta) \neq 0$ whenever $|\alpha - \beta| \le C$ for some constant $C > 0$. We choose our scattering phase function $K(\mathbf{x}, \alpha, \beta)$ to be a 2D Henyey–Greenstein function, which possesses the property mentioned above and is convenient to describe strongly forward-peaked scattering, according to [11].

All numerical tests were provided on the domain $\overline{\Omega}^h$ defined in section 4 on the uniform 100×100 grid (4.1),(4.2) with $a = 1, b = 3, d = 5$, $R = 1$; see (2.1), (2.2). We use the uniform grid for α as well:

$$-d = \alpha_0 < \alpha_1 < \cdots < \alpha_{M_\alpha} = d, \text{ where } M_\alpha = 50.$$

Similarly with [23], we apply a 2-step postprocessing procedure. Define $m = \max_{\mathbf{x}\in\Omega^h}(f_\delta^{comp}(\mathbf{x}))$. Then, the first step of the procedure removes undesirable artifacts by setting

$$\tilde{f}_\delta^{comp}(\mathbf{x}) = \begin{cases} f_\delta^{comp}(\mathbf{x}) & \text{if } f_\delta^{comp}(\mathbf{x}) > 0.2m, \\ 0 & \text{otherwise.} \end{cases}$$

In the second step, we smooth the obtained $\tilde{f}_\delta^{comp}(\mathbf{x})$ function out. For every grid point $\mathbf{x}$ of Ω^h, the value of $\tilde{f}_\delta^{comp}(\mathbf{x})$ at that point is replaced by the mean value $\hat{f}_\delta^{comp}(\mathbf{x})$ of the function over neighboring grid points. For brevity, we use $f_\delta^{comp}(\mathbf{x})$ notation instead of $\hat{f}_\delta^{comp}(\mathbf{x})$ below. In Tests 1–3 we display the exact functions $f_{true}(x, y)$ and computed functions $f^{comp}(x, y), f_\delta^{comp}(x, y)$ before and after the use of the postprocessing procedure.

6.2. Numerical results.

1. **Test 1. Circle-shaped smooth inclusion, no scattering.**
The function f_{true} is given by

$$f_{\text{true}}(\mathbf{x}) = \begin{cases} \exp(|\mathbf{x} - (0,2)|^2/(|\mathbf{x} - (0,2)|^2 - 0.3^2)), & |\mathbf{x} - (0,2)| < 0.3, \\ 0 & \text{otherwise.} \end{cases}$$

The function f_{true} is supported in the disk of the radius $r = 0.3$ with the center at the point $(x, y) = (0, 2)$. The graph of f_{true} is displayed in Figure 6.1(a).

$$\mu_s(\mathbf{x}) \equiv 0, \quad \mu_a(\mathbf{x}) = \begin{cases} 0.1 & \text{if } (x^2 + y^2) < 0.8, \\ 0 & \text{otherwise.} \end{cases}$$

The numerical solution for this case is displayed in Figure 6.1.

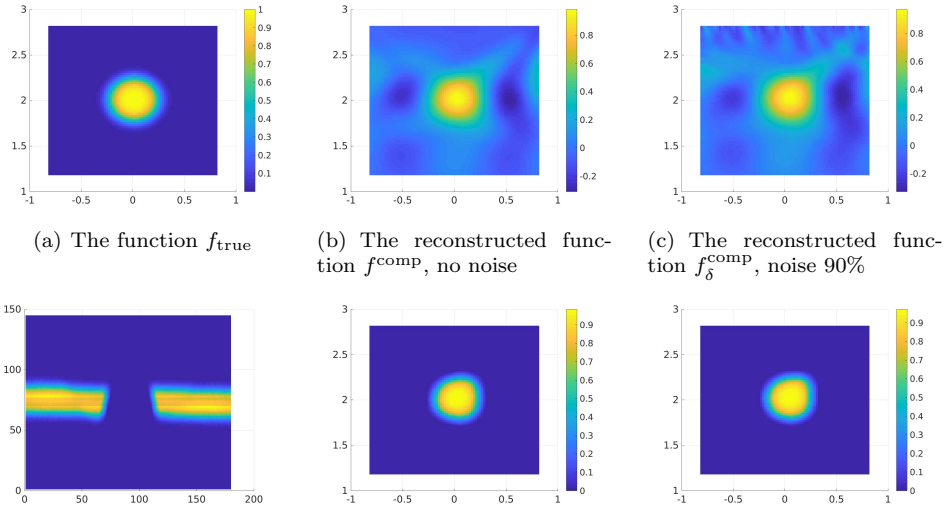

(a) The function f_{true} (b) The reconstructed function f^{comp}, no noise (c) The reconstructed function f_δ^{comp}, noise 90%

(d) The incomplete tomographic data, no noise (e) Postprocessed f^{comp}, no noise (f) Postprocessed f_δ^{comp}, noise level 90%

FIG. 6.1. *Test* 1. *The true and reconstructed source functions for circle-shaped smooth inclusion without scattering.*

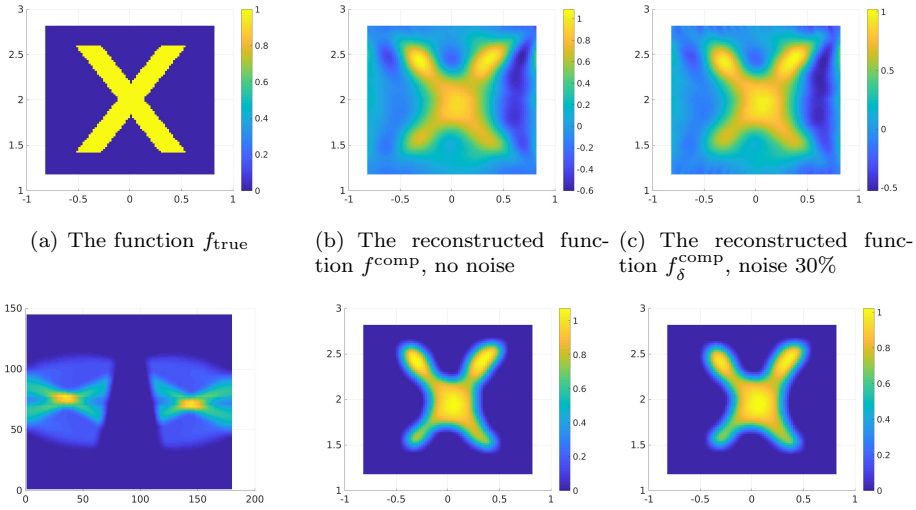

(a) The function f_{true} (b) The reconstructed function f^{comp}, no noise (c) The reconstructed function f_δ^{comp}, noise 30%

(d) The incomplete tomographic data, no noise (e) Postprocessed f^{comp}, no noise (f) Postprocessed f_δ^{comp}, noise level 30%

FIG. 6.2. *Test* 2. *The true and reconstructed source functions for X-shaped nonsmooth inclusion for the case of uniform scattering.*

2. **Test 2. X-shaped nonsmooth inclusion, uniform scattering.** The function f_{true} is depicted on the Figure 6.2(a). We define absorption and scattering coefficients as

$$\mu_a(\mathbf{x}) = \begin{cases} 0.1 & \text{if } (x^2+y^2) < 0.8, \\ 0 & \text{otherwise,} \end{cases} \quad \mu_s(\mathbf{x},\alpha) = \begin{cases} 0.01 & \text{if } (x^2+y^2) < 0.8, \\ 0 & \text{otherwise,} \end{cases}$$

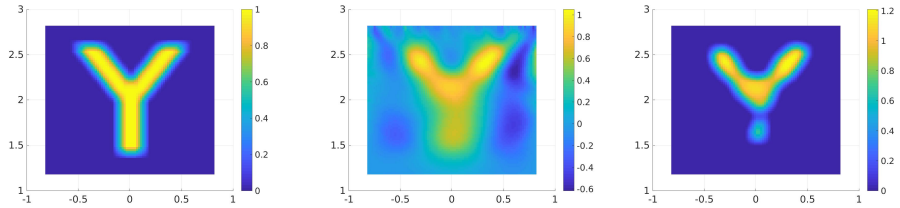

(a) The function f_{true} (b) The reconstructed function f_δ^{comp}, noise 60% (c) Postprocessed f_δ^{comp}, noise level 60%

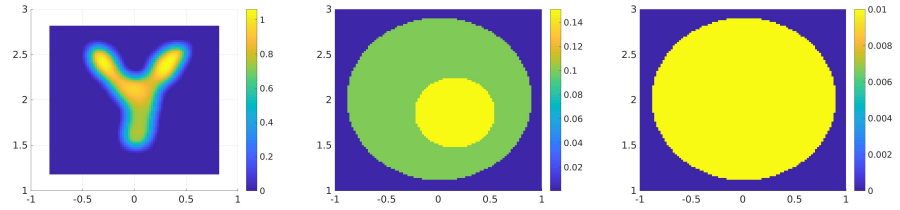

(d) Postprocessed f^{comp}, no noise (e) The absorption coefficient (f) The scattering coefficient

FIG. 6.3. *Test 3. The true and reconstructed source functions for Y-shaped inclusion for the case of strongly forward-peaked scattering.*

and the constant scattering phase function $K(\mathbf{x}, \alpha, \beta) = 1/(2d)$. The reconstruction is displayed in Figure 6.2.

3. **Test 3. Y-shaped inclusion, strongly forward-peaked scattering.** The function f_{true} depicted on Figure 6.3(a) is smooth and compactly supported in the domain. We define absorption and scattering coefficients as

$$\mu_a(\mathbf{x}) = \begin{cases} 0.15 & \text{if } (x,y) \in \text{supp}(f_{\text{true}}), \\ 0.1 & \text{if } (x^2+y^2) < 0.8, \\ 0 & \text{otherwise}, \end{cases}$$

and

$$\mu_s(\mathbf{x}) = \begin{cases} 0.01 & \text{if } (x^2+y^2) < 0.8, \\ 0 & \text{otherwise}, \end{cases}$$

and the scattering phase function

$$K(\mathbf{x}, \alpha, \beta) = H(\alpha, \beta) = \frac{1}{2d}\left[\frac{1-g^2}{1+g^2-2g\cos(\alpha-\beta)}\right], \tag{6.6}$$

where $H(\alpha, \beta)$ is the 2D Henyey–Greenstein function. In (6.6), $g = g(x, y)$ is the Henyey–Greenstein factor, it is the smoothed version of the function

$$\tilde{g}(x,y) = \begin{cases} 0.9 & \text{if } (x^2+y^2) < 0.8, \\ 0.5 & \text{otherwise}. \end{cases}.$$

The numerical solution for Test 3 is depicted on Figure 6.3.

Remark 6.1. In Tests 1 and 2, Figures 6.1(d) and 6.2(d) are given only for illustration purposes. They represent the incomplete Radon transform data, obtained by the well-known Radon transform of the function f^{true} in which case $\mu_a = \mu_s = 0$. The

case when the data are available for all $\mathbf{x}$ and $\mathbf{x}_\alpha$ such that the set of lines $L(\mathbf{x}, \mathbf{x}_\alpha)$ contains all possible lines intersecting domain Ω is considered to be the tomographic inverse problem with complete data. In contrast to this, we study the case when, the point source $\mathbf{x}_\alpha$ runs along the straight line as shown in Figure 2.1. In that scenario, the data in our problem are said to be incomplete and Figures 6.1(d) and 6.2(d) illustrate this. In Test 3 we omit the image representing incomplete Radon data, for the reason that it does not differ qualitatively from Figures 6.1(d) and 6.2(d), while the distributions of the absorption and scattering coefficients differ significantly from the previous two tests.

7. Appendix.

THEOREM 7.1 (uniqueness and existence of the solution of the forward problem). *Consider a rectangular domain Ω, defined in* (2.1). *Assume that functions $f, \mu_a, \mu_s \in C^1(\mathbb{R}^2), f \in L^2(\mathbb{R}^2)$, and the function $K \in C^1(\mathbb{R}^2 \times [-d,d]^2)$. Also, assume that* (2.4) *holds. Then there exists a unique solution $u(\mathbf{x}, \alpha)$ of Problem* 2.1 *in the domain Ω such that $u(x, y, \alpha) \in C^1(\mathbb{R} \times [0, b] \times [-d, d])$. Furthermore, $u(x, y, \alpha) = 0$ for $y \in (0, a)$ as well as for sufficiently large $|x|$.*

Proof. Let $L(\mathbf{x}, \mathbf{x}_\alpha)$ be the segment of the straight line connecting points $\mathbf{x}$ and $\mathbf{x}_\alpha$. Then for any appropriate function $\phi(\mathbf{x})$

$$\int_{L(\mathbf{x},\mathbf{x}_\alpha)} \phi(\boldsymbol{\xi}) ds_{\boldsymbol{\xi}} = \frac{|\mathbf{x} - \mathbf{x}_\alpha|}{y} \int_0^y \phi\left(\alpha + \frac{w(x-\alpha)}{y}, w\right) dw,$$

where $ds_{\boldsymbol{\xi}}$ is the arc length. It follows from (2.1)–(2.4) that $u(\mathbf{x}, \alpha) = 0$ for $y \in (0, a)$. Therefore, the forward problem in the domain Ω is equivalent to

$$u(\mathbf{x}, \alpha) = \chi^{-1}(\mathbf{x}, \alpha) \frac{|\mathbf{x} - \mathbf{x}_\alpha|}{y} \int_a^y \chi(\mathbf{z}) \mu_s(\mathbf{z}) \int_{-d}^d K(\mathbf{z}, \alpha, \beta) u(\mathbf{z}, \beta) d\beta dw + \chi^{-1}(\mathbf{x}, \alpha) \frac{|\mathbf{x} - \mathbf{x}_\alpha|}{y} \int_a^y (f\chi)(\mathbf{z}) dw \tag{7.1}$$

and

$$\mathbf{z}(w, x, \alpha) = \left(\alpha + \frac{w(x-\alpha)}{y}, w\right), \quad \ln \chi(\mathbf{x}, \alpha) = \frac{|\mathbf{x} - \mathbf{x}_\alpha|}{y} \int_0^y (\mu_a + \mu_s)(\mathbf{z}) dw. \tag{7.2}$$

Estimate from below the absolute value of the first argument in $\mathbf{z}(w, x, \alpha)$ in (7.2). By (2.1), (2.4), and (7.2) the left-hand side of (7.1) is not zero only if $y \in (a, b)$. Since in $\mathbf{z}(w, x, \alpha)$ we have $w \in (a, y), \alpha \in (-d, d)$, then

$$\left|\alpha + \frac{w(x-\alpha)}{y}\right| \geq \frac{w}{y} |x - \alpha| - |\alpha| \geq \frac{a}{b} |x| - \left(1 + \frac{a}{b}\right) |\alpha| \geq \frac{a}{b} |x| - \left(1 + \frac{a}{b}\right) d. \tag{7.3}$$

Suppose that $|x| \geq X$ and X is so large that $1 - \frac{1}{X}(1 + \frac{b}{a})d > \frac{1}{2}$, $\frac{a}{2b} X > R$. Then (7.3) implies that $|\alpha + w(x-\alpha)/y| > R$. Hence, by (2.1) and (7.2) the right-hand of (7.1) equals zero for $|x| \geq X$. Let

$$A(u) : C\left(\mathbb{R}^2 \times [-d, d]\right) \to C\left((|x| \leq X) \times [-d, d] \times [-d, d]\right)$$

be the operator in the right-hand side of (7.1). Then (7.1) can be considered as the equation $u = A(u)$ with the Volterra-like integral operator, where the "Volterra

property" is due to the integration with respect to y. Therefore, the latter equation can be solved iteratively, as is usually done for the Volterra integral equations. It is obvious from the above discussion that all iterates $A(u_n)(\mathbf{x},\alpha) = 0$ for $|x| \geq X$. Thus, the solution of (7.1) in the space $C(\mathbb{R}^2 \times [-d,d])$ exists and is unique. The C^1-smoothness of this solution with respect to x, y, α obviously follows from the well-known convergence estimate for the iterates of a Volterra integral equation. Due to the above-mentioned equivalence, this implies uniqueness and existence of the solution of the forward problem. ∎

The numerical solution of the forward problem was performed via the iterative solution of the Volterra-like integral equation (7.1) for $(\mathbf{x},\alpha) \in (|x| \leq X) \times [a,b] \times [-d,d]$.

REFERENCES

[1] M. A. Anastasio, J. Zhang, D. Modgil, and P. J. La Rivière, *Application of inverse source concepts to photoacoustic tomography*, Inverse Problems, 23 (2007), pp. S21–S35.

[2] A. B. Bakushinsky, M. Yu. Kokurin, and A. Smirnova, *Iterative Methods for Ill-Posed Problems: An Introduction*, de Gruyter, Berlin, 2011.

[3] G. Bal and A. Tamasan, *Inverse source problems in transport equations*, SIAM J. Math. Anal., 39 (2007), pp. 57–76.

[4] L. Baudouin, M. de Buhan, and S. Ervedoza, *Convergent algorithm based on Carleman estimates for the recovery of a potential in the wave equation*, SIAM J. Numer. Anal., 55 (2017), pp. 1578–1613.

[5] L. Beilina and M. V. Klibanov, *Approximate Global Convergence and Adaptivity for Coefficient Inverse Problems*, Springer, New York, 2012.

[6] M. Bellassoued and M. Yamamoto, *Carleman Estimates and Applications to Inverse Problems for Hyperbolic Systems*, Springer, Tokyo, 2017.

[7] L. Bourgeois and J. Dardé, *A duality-based method of quasi-reversibility to solve the Cauchy problem in the presence of noisy data*, Inverse Problems, 26 (2010), 095016.

[8] L. Bourgeois, D. Ponomarev, and J. Dardé, *An inverse obstacle problem for the wave equation in a finite time domain*, Inverse Probl. Imaging, 13 (2019), pp. 377–400.

[9] A. L. Bukhgeim and M. V. Klibanov, *Uniqueness in the large of a class of multidimensional inverse problems*, Sov. Math. Dokl., 17 (1981), pp. 244–247.

[10] J. P. Guillement and R. G. Novikov, *Inversion of weighted Radon transforms via finite Fourier series weight approximation*, Inverse Probl. Sci. Eng., 22 (2013), pp. 787–802.

[11] J. Heino, S. Arridge, J. Sikora, and E. Somersalo, *Anisotropic effects in highly scattering media*, Phys. Rev. E(3), 68 (2003), 03198.

[12] V. Isakov, *Inverse Problems for Partial Differential Equations*, 3rd ed., Springer, New York, 2017.

[13] M. Jiang, T. Zhou, J. Cheng, W. Cong, and G. Wang, *Image reconstruction for bioluminescence tomography from partial measurement*, Opt. Express, 15 (2007), pp. 11095–11116.

[14] S. I. Kabanikhin, A. D. Satybaev, and M. A. Shishlenin, *Direct Methods of Solving Inverse Hyperbolic Problems*, VSP, Utrecht, 2005.

[15] M. V. Klibanov, *Inverse problems and Carleman estimates*, Inverse Problems, 8 (1992), pp. 575–596.

[16] M. V. Klibanov and A. Timonov, *Carleman Estimates for Coefficient Inverse Problems and Numerical Applications*, Inverse Ill-posed Probl. Ser., VSP, Utrecht, 2004.

[17] M. V. Klibanov, *Carleman estimates for global uniqueness, stability and numerical methods for coefficient inverse problems*, J. Inverse Ill-Posed Probl., 21 (2013), pp. 477–560.

[18] M. V. Klibanov and N. T. Thành, *Recovering dielectric constants of explosives via a globally strictly convex cost functional*, SIAM J. Appl. Math., 75 (2015), pp. 518–537.

[19] M. V. Klibanov, *Carleman estimates for the regularization of ill-posed Cauchy problems*, Appl. Numer. Math., 94 (2015), pp. 46–74.

[20] M. V. Klibanov, *Convexification of restricted Dirichlet to Neumann map*, J. Inverse Ill-Posed Probl., 25 (2017), pp. 669–685.

[21] M. V. Klibanov, A. E. Kolesov, A. Sullivan, and L. Nguyen, *A new version of the convexification method for a 1-D coefficient inverse problem with experimental data*, Inverse Problems, 34 (2018), 115014.

[22] M. V. Klibanov, J. Li, and W. Zhang, *Electrical impedance tomography with restricted Dirichlet-to-Neumann map data*, Inverse Problems, 35 (2019), 35005.
[23] M. V. Klibanov and L. H. Nguyen, *PDE-based numerical method for a limited angle X-ray tomography*, Inverse Problems, 35 (2019), 045009.
[24] A. D. Klose, V. Ntziachristos, and A. H. Hielscher, *The inverse source problem based on the radiative transfer equation in optical molecular imaging*, J. Comput. Phys., 202 (2005), pp. 323–345.
[25] R. Lattes and J. L. Lions, *The Method of Quasireversibility: Applications to Partial Differential Equations*, Elsevier, New York, 1969.
[26] Q. Li and L. H. Nguyen, *Recovering the initial condition of parabolic equations from lateral Cauchy data via the quasi-reversibility method*, preprint, https://arxiv.org/abs/1902.07637, 2019.
[27] A. K. Louis, *Incomplete data problems in x-ray computerized tomography*, Numer. Math., 48 (1986), pp. 251–262.
[28] F. Natterer, *The Mathematics of Computerized Tomography*, Classics Appl. Math. 32, SIAM, Philadelphia, 2001.
[29] F. Natterer, *Inversion of the attenuated radon transform*, Inverse Problems, 17 (2001), pp. 113–119.
[30] L. H. Nguyen, Q. Li, and M. V. Klibanov, *A convergent numerical method for a multi-frequency inverse source problem in inhomogenous media*, Inverse Probl. Imaging, 13 (2019), pp. 1067–1094.
[31] R. G. Novikov, *An inversion formula for the attenuated X-ray transformation*, Ark. Mat., 40 (2002), pp. 145–167.
[32] A. A. Samarskii, *The Theory of Difference Schemes*, Marcel Dekker, New York, 2001.
[33] A. J. Silva Neto and M. N. Özişik, *An inverse problem of simultaneous estimation of radiation phase function, albedo and optical thickness*, J. Quant. Spectrosc. Radiative Transfer, 53 (1995), pp. 397–409.
[34] P. Stefanov and G. Uhlmann, *An inverse source problem in optical molecular imaging*, Anal. PDE, 1 (2008), pp. 115–126.
[35] A. N. Tikhonov, A. V. Goncharsky, V. V. Stepanov, and A. G. Yagola, *Numerical Methods for the Solution of Ill-Posed Problems*, Kluwer, London, 1995.